4 Analysis of E-field Strength with the Near-Field of a HF Antenna

4.1 Introduction

This chapter aims to assess the near-field characteristics in compliance with the ICNIRP exposure levels. In this chapter, the influential parts of a high power HF broadcasting curtain array antenna and its ground environment are addressed. Their impact on the near-field electric field distribution is also described in this chapter.

This chapter is divided into three parts. Firstly it discusses the factors which have a potential impact on the distribution of the near-field. It then discusses a modeling protocol for future transmission site surveys. This will help further simplify the modeling and computation requirements for human exposure in the vicinity of high power short-wave broadcasting sites.

As shown in the pictures of Vantican Radio (Vantican) and Skelton (Cumbria UK) in Chapter 2, underneath the array and in the vicinity of the transmitter sites the ground environments are very complex. These high power broadcast antennas and transmission sites vary from one to another. Field measurements in the preliminary investigation showed that the field distributions were much more complicated than those predicted in the basic antenna model considering only the dipole array. Only considering the EMF radiated by the antenna itself will not be adequate or realistic when considering human exposure to such an intensive electric field. Therefore, a series of scenarios of a chosen broadcast array were considered to investigate the potential influential factors in order to assess its near-region EMF. The process of modelling also provides efficient guidance and references to apply to a wide range of sites. Chapter 3 studied the various effects that parameter variations can have on the Whole-body Average Specific Absorption Rate (WBSAR). WBSAR is an international metric of basic restriction for human exposure [4.1], which is largely dependent on the frequency of the incident wave. This was achieved through simulation and calculation using high resolution anatomical human voxel phantoms and the Finite Differential and Time Domain (FDTD) method. The studies in chapter 3 have shown how the

whole-body average SAR correlates with external electric field strength and its corresponding ICNIRP basic exposure limits and reference level. This chapter focuses on studying the ground and infrustructure's impacts on reflection and scattering of the incident field.

4.2 Modelling of the antenna radiating element

The BBC 'Skelton C' HF curtain array is shown in Fig 4.1 and has been modelled using both Method of Moments (MoM) [4.2] and the Finite Integration Technique (FIT) [4.3]. Simulation models were built in MoM based NEC4, while CST microwave studio is based on FIT methods. Both numerical methods and associated computational software were introduced in Chapter 2. The reasons for using these two software packages and comparisons with other popular commercial electromagnetic simulators were also described previously.

a) Curtain array b) feeder and splitter

Fig 4.1 BBC Skelton C broadcasting transmission site, HF curtain array.

A typical curtain array consists of an array of folded/cage/box dipoles. The dipole elements are centre fed with a 300-ohm balanced transmission line. The HF broadcasting antennas are mainly horizontally polarised. The folded/cage/box dipoles are seen as dipole elements of the array. They were either arranged vertically in stacks or horizontally in bays. The Babcock Skelton C transmission site HF curtain array 766 is a typical HRS 4/5/0.5λ array and is used as the research template for this work. "HRS" is a standard nomenclature in the broadcasting industry. It indicates that the array is beam slewable, horizontally polarized and incorporates a reflector. Skelton C curtain array 766 has 4 dipoles in a row and 3 in each column, or can be described as 4

bays and 3 stacks. As shown in Fig 4.1 each box shape dipole element of the Skelton C array 766 is a wideband folded dipole. Each dipole element is 19.6m long and 2.5m wide. The lowest row of dipoles is mounted 0.5λ above the ground, where λ is the wavelength at the design frequency. In this case, the Skelton C array 766 is designed and operated at up to 399kW and in the 6-7 MHz frequency band, meaning the lowest dipole elements are about 23 metres above the ground. The adjacent dipole element columns have a spacing of about 2.5m. The reflecting screen consists of 100 horizontal wires, which are spaced 0.758m apart and are mounted stacked up vertically. They are supported by catenary wires and placed approximately 10m behind the plane of dipoles.

Considering the geometry of a 6-7MHz HF curtain array, a model could be very large. The reflectors are 110m by 12m; the two 90m high supporting towers have a 15m x15m wide base, all of which can be seen in Fig 4.1. The high power HF broadcasting system is comprised of the array and the scatterers. The supporting and ground infrastructure is electrically large and complex. The effects of this structure on the near-field EMF has not been considered in other studies. However, their effects cannot be overlooked when the antenna output power is up to a few hundred kW.

In order to understand and analyse the near-field characteristics, assembly modelling strategies to tackle electromagnetically large computational problems are required. There are various suitable numerical methods for different modelling requirements, and the computational methods to conduct this study were compared and described in chapter 2. The complexity of the model for the transmitting antenna can become impractical for such complex and large structures. In Numerical Electromagnetics Code 4 (NEC4) wire antennas [4.4] were modelled as short, straight segments. The wire segmentation geometrically followed the antenna element coordinates of two end points and its radius. The segment length was defined relative to a fraction of the wavelength (λ) at the desired frequency and should be less than a tenth of the wavelength. Compared with Finite Differential Time Domain (FDTD) and other 3D EM simulation methods, the computer time and resources required by the Moment of Method are relatively small. It is obviously desirable to reduce the computational demmands of a very large modelling problem without sacrificing the accuracy of the result. However NEC-4 is limited to a maximum of 12000 segments. The key to

transmitter site modelling is to identify the most influential components and their effects on the EMF in the near field region.

Prior to modelling the entire HF curtain array, a single element was simulated to ensure the validity of the calculated E-field distributions in both NEC and CST which are shown in Fig 4.2a-b.

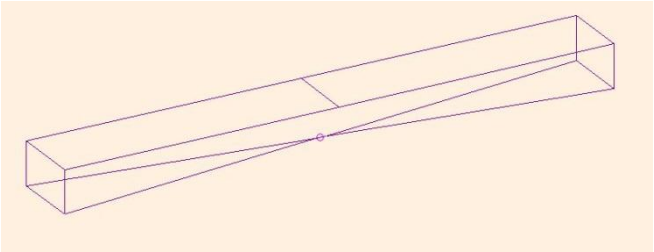

a) Box shaped folded dipole array element model in NEC4

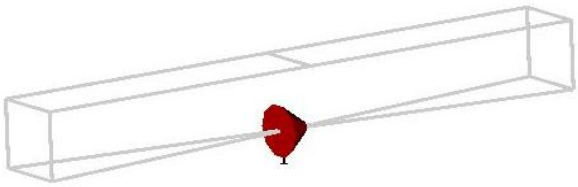

b) Box shaped folded dipole array element model in CST microwave studio

Fig 4.2 Skelton curtain array single element[1] in NEC 4 and CST microwave studio.

The simulation was performed using both the MoM and FIT methods. In CST, which used the FIT method, the antenna was modelled using 9 and 15 segments per half-wavelength models. In NEC4, which uses the MoM, the antenna was modelled using 10 and 20 lines per wavelength. The simulated results in Fig 4.3 showed a good level of agreement between both EM simulators. NEC4 is an efficient and accurate technique; well-known for modelling wires and linear dielectrics. CST microwave studio can handle complex inhomogeneous geometries such as the human body but are very expensive and time consuming for large electrical radiation problems. In fact none of the commercial codes currently available are well-suited to the electromagnetic problem studied in this thesis. Therefore, CST microwave studio was used to verify the results of NEC4 model. It was also considered to calculate the human SAR in a full scale HF transmitting site with a human voxel phantom placed in front of the array.

[1]Courtesy, Babcock Skelton transmission site, Perith, Cumbria and Marconi

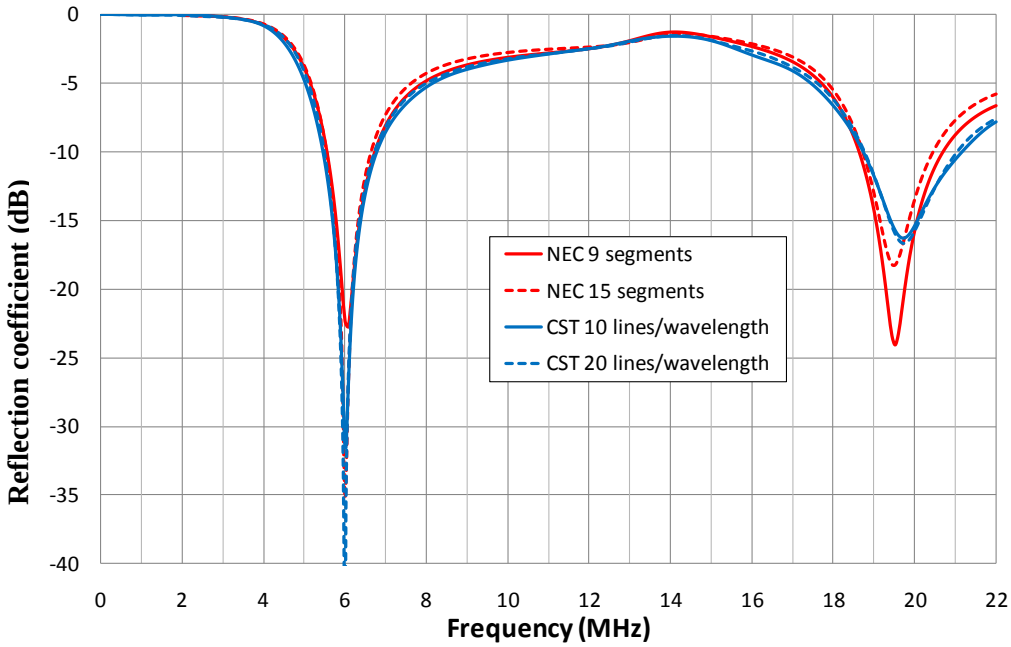

Fig 4.3 Simulated reflection coefficient of a single element of the HF curtain array.

The box dipole element is resonant at its designed 6MHz frequency. When a high power HF broadcasting curtain array is operating at full power (up to 500kW), it should be able to deliver its rated power to a load where the VSWR is required to be better than 1.5:1 across the operating band [4.5]. Equivalently the Return Loss of an array needs to above 14dB. Both the NEC and CST models predict return loss values above 20dB. In order to model the worst case human exposure a balanced network was employed. Additionally it was assumed that the antenna was well matched so that all of the power delivered to the antenna is radiated efficiently.

4.3 Analyses of antenna complexity

Due to the nature of the complex mechanical configuration and the size of the HF curtain array, a highly detailed and precise model is impractical and unnecessary. The highest point of the tower can be as much as 100m above the ground and the highest elements of the array can be 70m above ground. There are numerous wires and components. Meanwhile, there is a maximum number of total segments that can be processed in NEC and the number of meshes in CST is directly linked to the hardware resources and computational time required. 3D EM numerical computational methods require an increased computing time along with more powerful hardware such as

multi-core/CPUs and graphics processing units (GPUs). Therefore, it is necessary to determine an efficient modelling protocol to ensure an accurate simulation.

Breaking the complex problems down to multiple steps and parts assisted the studies of their impacts on the reflection and scattering of the incident field. This was necessary to establish an assessment methodology which would be able to be applied in a wide range of HF human RF exposure compliance invistagations. However, the process of assessing the incident field within an electrically large and complex struture is still time consuming and the accuary is questionable. The staff at the BBC Skelten C tranimission site kindly provided the orignial drawing of the broadcasting curtain array, the supporting tower and ground from its designer-Marconi company. Then two levels of complexity models based on the array were built in NEC4. They were a most detailed one and a simplified one. Later the ground topography and ground metal infrastructures were considered and added to form a whole broadcasting array for analysing the near-region EMF. Apart from conventional numerical methods, an equivalent principle implementation can be used as an alternative solution. This can dramatically reduce the computational time and complexity of the modelling exercise. The hybird (Equivalent Principle – FDTD) approach will be given detailed analysis in chapter 5.

A model of this antenna configuration was built in NEC4. The same geometry model was also imported into CST microwave studio. The numerical theories of these computational methods were briefly given in Chapter 2. Firstly the Skelton HF array was modelled, including the main simplified curtain array and reflectors, as shown in Fig 4.4a. Secondly the main curtain array structure and other supports were modelled at each side of the array, using the same distance which was given by the Skelton C Marconi installation drawings.

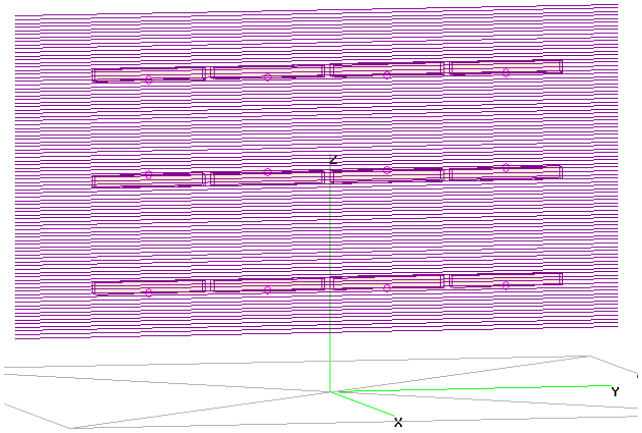

a)

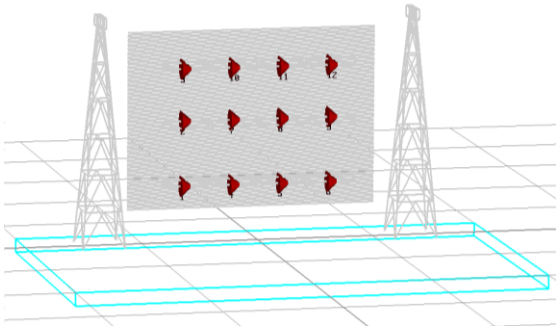

b)

Fig 4.4 Skelton C HF curtain array with reflectors and supporting towers:
a) 4x3 array model in NEC4 b) Array model in CST with ground and supporting towers.

The tower structure was a typical self-supporting metal mast. Fig 4.4a shows the first model built in NEC4. The ground conditions can be modified accordingly. It also incorporates the details of the supporting mast structures. Compare this with the much simpler model as shown in Fig 4.4b. The simulations results show that both models produce a similar EMF distribution. Therefore the complexity of the supporting mast structure does not significantly affect the E-field distribution in the lower ground.

The simplified model (Fig 4.4a) was modelled in NEC 4, it has a take-off angle of 15 ° and a gain of 20dBi over a perfect conducting flat plane. The curtain array radiation patterns show that the array has -3dB beamwidth of 20 °. The results agree well with the International Telecommunication Union (ITU) Recommendation ITU-R BS.80-3 [4.6] on transmitting directional narrow horizontal beamwidth curtain antennas (HRS 4/3/h, where $0.4\lambda \leq h \leq 1.5\lambda$) in HF broadcasting. The HF broadcasting area is approximately greater than 2000 km from the antenna (far field). This validated the simplified model of the Skelton C curtain array antenna 766. The human occupational

and public exposure would be evaluated in the direction of the maximum of the radiation pattern (the x-axis of the model and simulation results in this thesis is aligning to the propagation direction). The EMF in the direction of side lobes was found to be much weaker, meaning it is not a concern. The components of the curtain array, reflecting screen, feeder bay, supporting masts and other ground infrastructure are mainly metal with numerous details. The curtain array, feeders and reflector screen are supported by a pair of self-supporting towers and guy wire systems, shown in the plan view Fig 4.5a and front view Fig 4.5b. Both the towers and ground-anchored guy-wires are grounded by attaching to an anchor; a metal rod with an eyelet and steel plate cemented into a hole or buried in the earth diagonally perpendicular to the angle of the guy wire [4.7], [4.8].

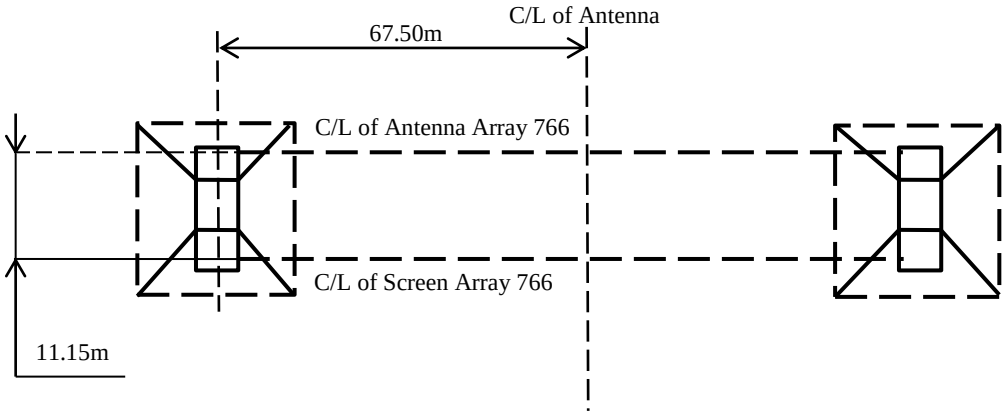

a) Plan view

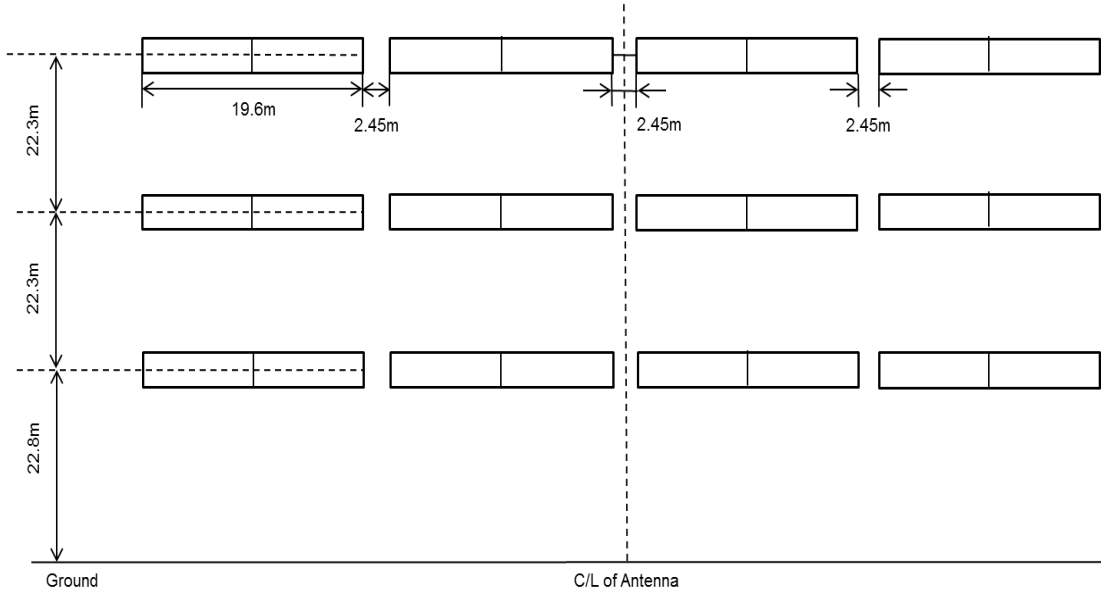

b) A front overview of Skelton C curtain array 766.

Fig 4.5 Schematic of the Skelton C curtain array antenna 766 (Type R9010, HRS 4/3/0.5λ) for 6/7 MHz.

As the self-supporting towers were not included in the Marconi installation drawings, the effects of the towers on the EMF were not clear. Therefore two wire models for the supporting towers with differing complexity have been simulated in NEC4, as shown in Fig 4.6. All the models contained all of the dipole elements and the reflecting screen. Other ground infrastructures have been gradually included into the models and simulated; the effects will be discussed in the following sections of this chapter.

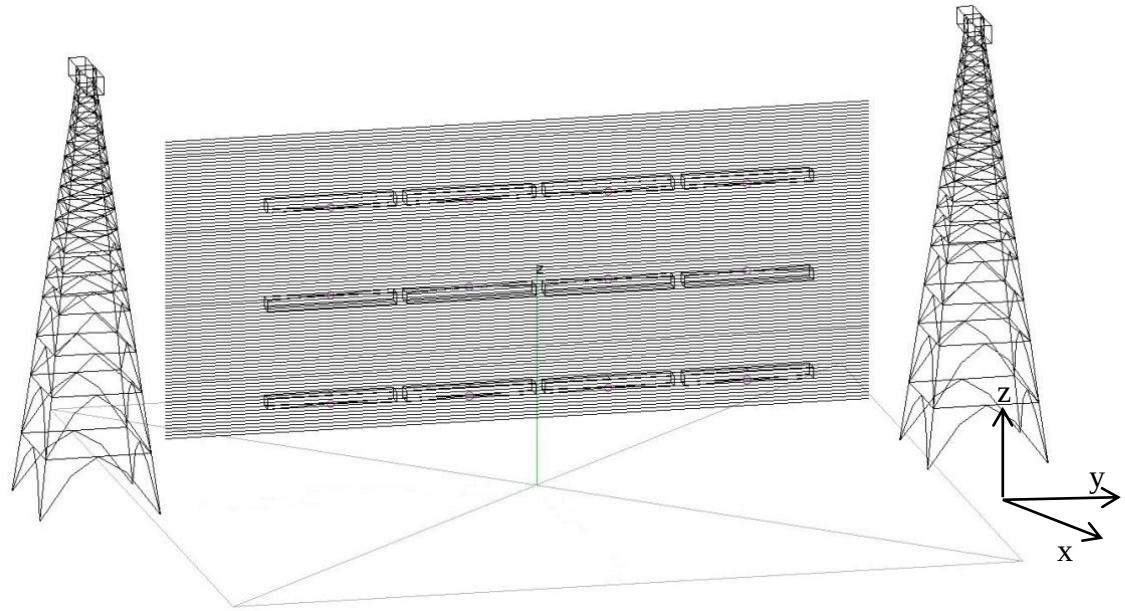

a) Normal Supporting towers model

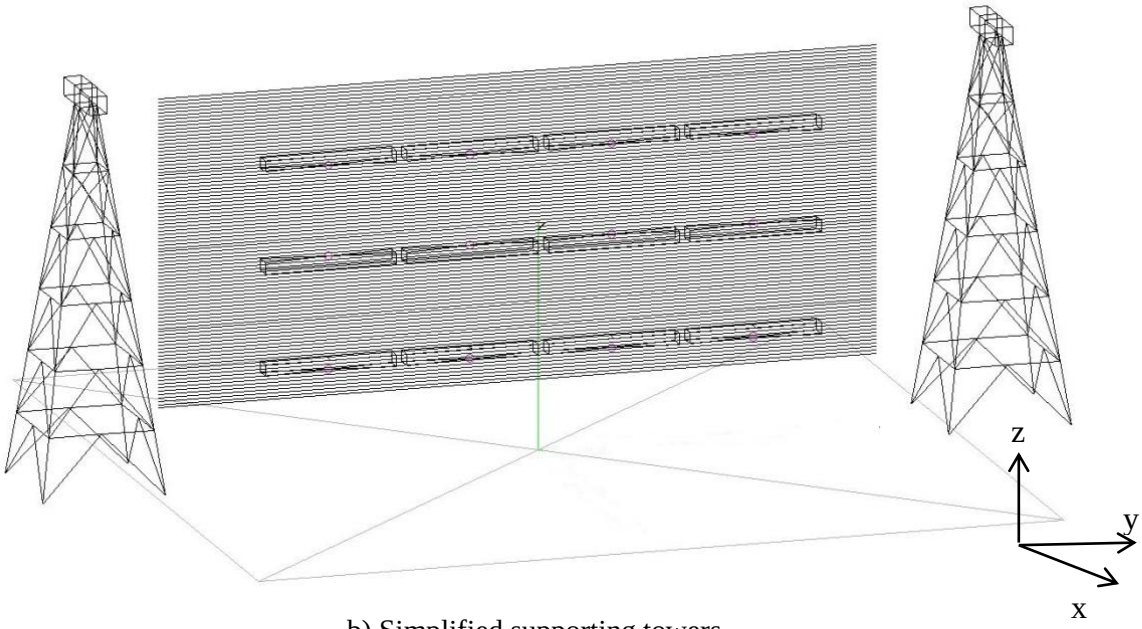

b) Simplified supporting towers

Fig 4.6 Two supporting tower models.

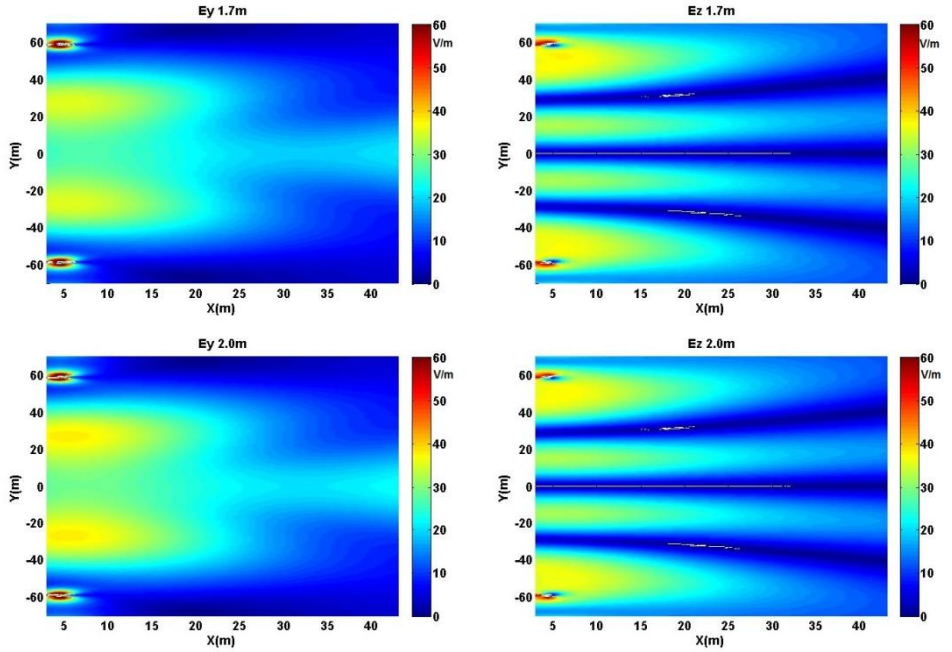

a) Normal towers and array 300kW

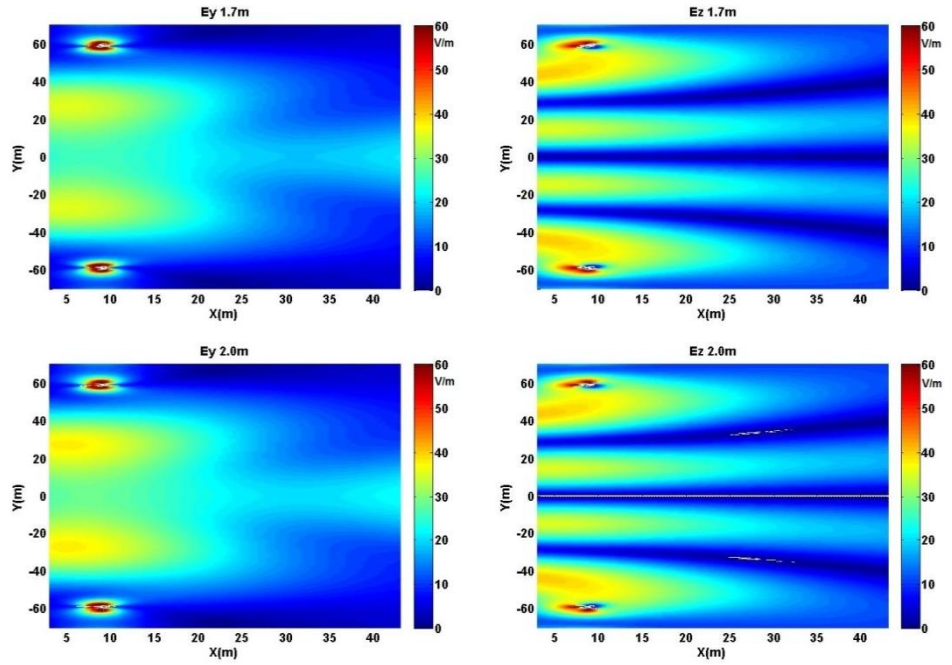

b) Simplified towers and array 300kW

Fig 4.7 Near-field distribution with different supporting tower models over average lossy ground with dielectric properties of $\varepsilon_r = 13$ and $\sigma = 0.005$ S/m.

The models displayed in Fig 4.6a-b feature tower heights of 99m and 89m, respectively. The base sizes of the towers are the same geometry but with different levels of detail on the structures. Comparison of Fig 4.7a-b shows that the field value and patterns were not affected by the detail change of the towers' models. The main EMF distribution has not been disturbed much. The level of E-field value remains the

same in front of the array and the highest E-field value still appears in the region of the towers. The model in Fig 4.7b was chosen for the primary Skelton C curtain array 766 and supporting towers model. Other potential influential factors will be presented in following sections of this chapter.

The near-field E-field of a HF transmitting antenna is far from uniform. Humans are more sensitive to the vertical E-field component. Compared with the field distribution in front of MF broadcast antennas the variation appears in both vertical and horizontal E-field components. The induced current densities in human bodies caused by incident EMF are influenced by the polarization and levels of the time varying EMF and the human body itself. Considering a human standing with arms stretched out in the EMF, their body naturally acts as a 'T' monopole which increases the coupling to a horizontal E-field (Ey). Since there is no complementary image present, the ground effect coupling is less. The wrist and ankle region have the smallest cross-sectional area of a human body. The average current density induced by the incident antenna field appears higher in both regions, as results show in the previous chapter. Furthermore both wrists and ankles consist mainly of bones and tendons with little high-conductivity muscle. Current flow through the muscles of both regions will cause high levels of localised SAR due to the high conductivity muscle and narrow cross-sectional area. In this case, while the whole-body averaged SAR does not necessarily appear to exceed the limits, the localised SAR in the ankle and wrist regions are the most restrictive quantities. Therefore, ankle and wrist currents would be used to assess the exposure levels against ICNIRP limits. By using an ankle current meter, a direct measurable quantity can be linked to the energy absorbed by human bodies. Therefore, the cross-polar (Ez) and co-polar (Ey) incident E-field are considered at two heights in the primary investigation: 0.2m or ankle height and 1.7m or shoulder height (outstretched arms height).

Due to the limits on the number of points NEC can calculate and the area that needed to be investigated in front of the array (up to 70m wide and 70m long in front of the array) the E-field was first sampled at 1 m intervals. However, this proved inadequate. The E-field strength values were then calculated and mapped at 0.5m intervals in both the x and y axis directions. The height above the ground (z-axis) was chosen to be 0.2m and 1.7m, which showed clear results and was also efficient. But the processes

were still quite time consuming, because for each simulation to plot 90mx70m E-field values at two z planes in 0.5m intervals requires 45522 total field points and a full model needed to run for about 4 hours by an Intel Quad Core CPU Q8300 (2.50GHz) with 4GB RAM. The same antenna model in CST microwave studio on the same computer needed about 3 hours to finish each simulation, but the calculated field points are dependent on the meshing of the model. The height of the average human ankle is considered to be 0.2m above the ground, while 1.7m is considered as a typical height of an adult male. Later 0.5m and 2.0m height field distributions were also considered in studies to verify the variations level.

4.4 Ground characteristics of HF transmission sites

The geometrically identical models of the array have been simulated using both NEC4, and CST Microwave Studio. Two different ground scenarios were considered for each numerical method; the array located above a perfect electric conducting ground and above a lossy ground (average ground condition). In CST Microwave Studio, a tenth of the wavelength (frequency at 6MHz) i.e. 5m thick brick was modelled in order to represent a more realistic ground condition. Initial ground slabs were modelled using permittivity and conductivity values of $\varepsilon_r = 13$ and $\sigma = 0.005$ S/m, which are the same as those used in the NEC4 implemented Sommerfeld solution for the average lossy ground condition. In this thesis, the average lossy ground was abbreviated as average ground (AVG). The effects of ground thickness on simulation and human coupling have been discussed in Chapter 3.

Simulations were performed at 6MHz with excitation powers of 1W and 300kW. All field values in this study are presented in V/m. In the very close region of the transmitting array (within one wavelength in front of the antenna), high levels of EMF would still be expected. The effects of the ground reflection on the EMF and human body should not be overlooked. In this chapter, the lossy ground condition was compared with a perfect electrically conducting ground. Results with and without the self-supporting towers are also included in these comparisons. The results are as follows:

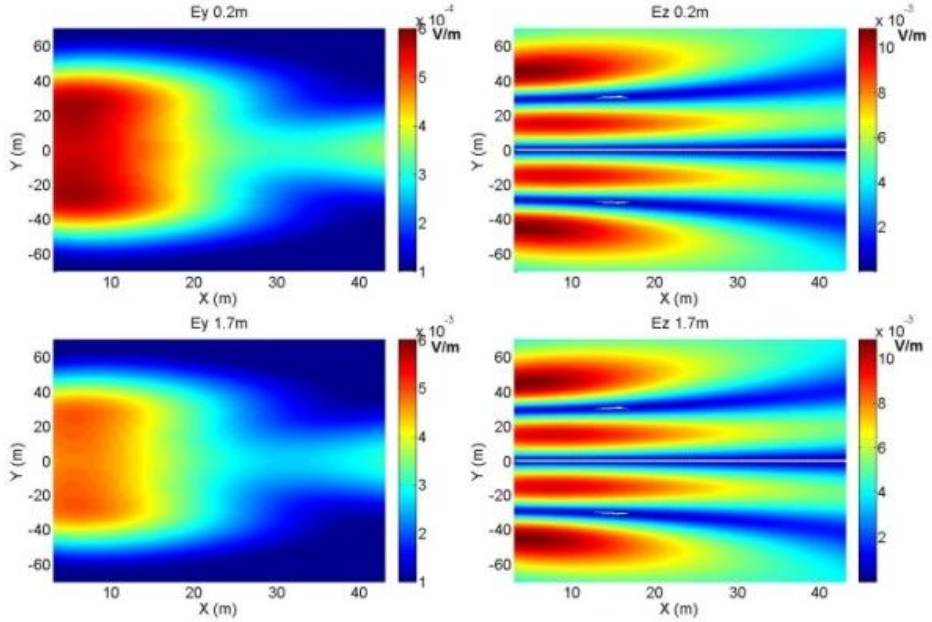

a) Near-field distributions calculated in NEC4

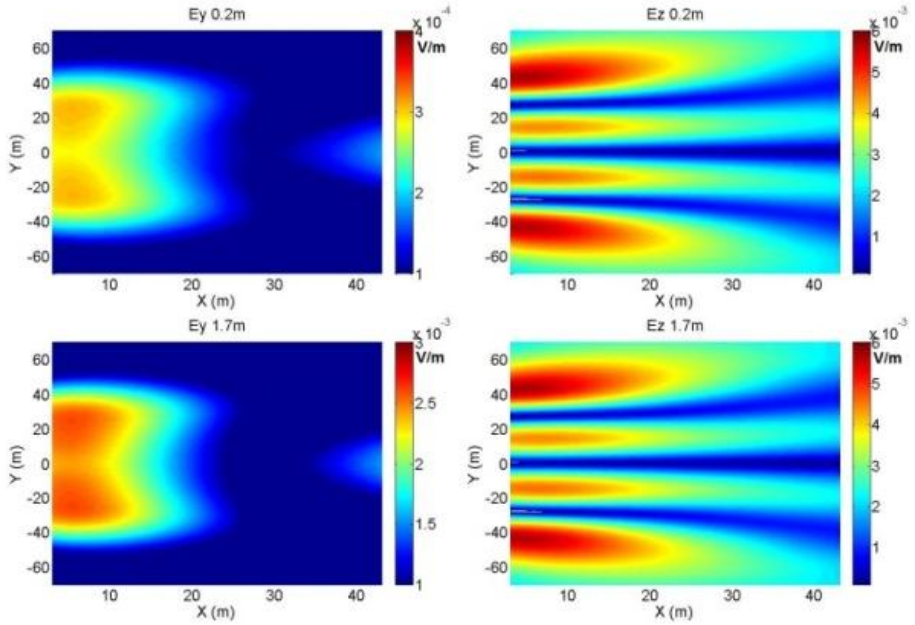

b) Near-field distributions calculated in CST

Fig 4.8 Array E-field without supporting towers above a perfect electrical ground (1W).

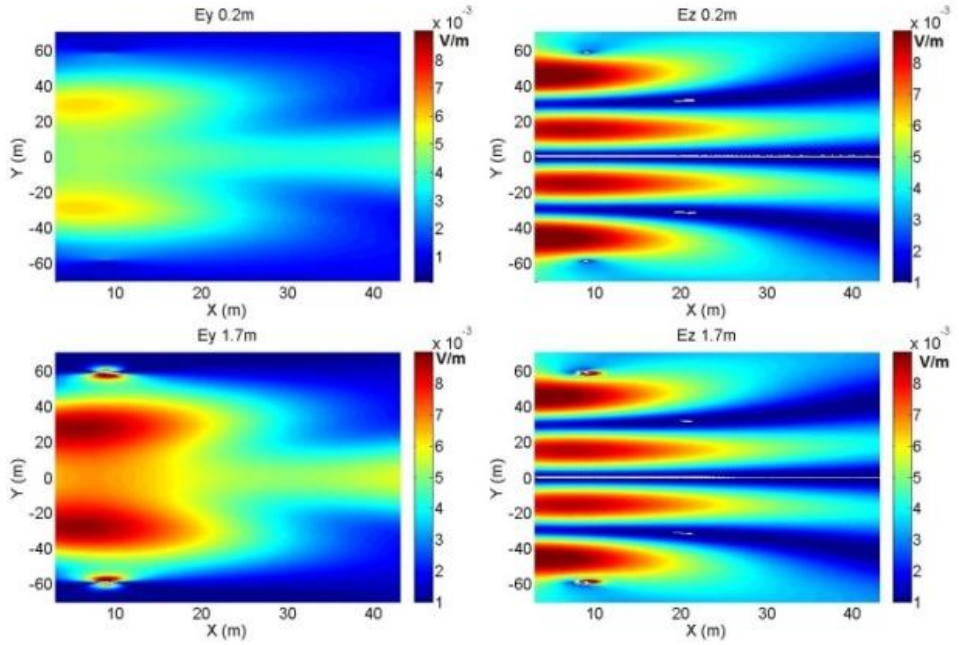

a) Near-field distributions calculated in NEC4

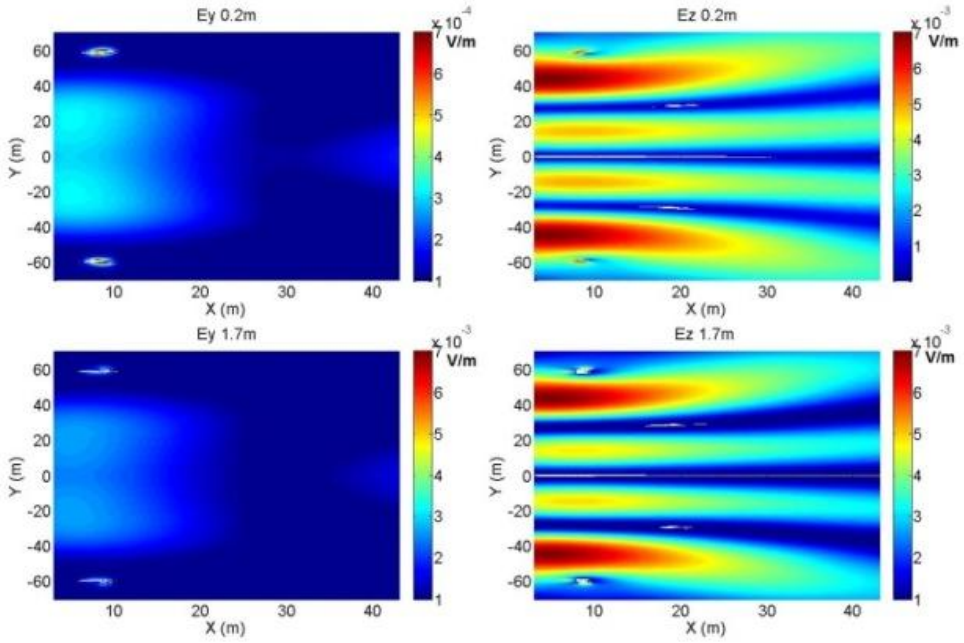

b) Near-field distributions calculated in CST.

Fig 4.9 Array E-field with supporting towers above a perfect electrical ground (1W).

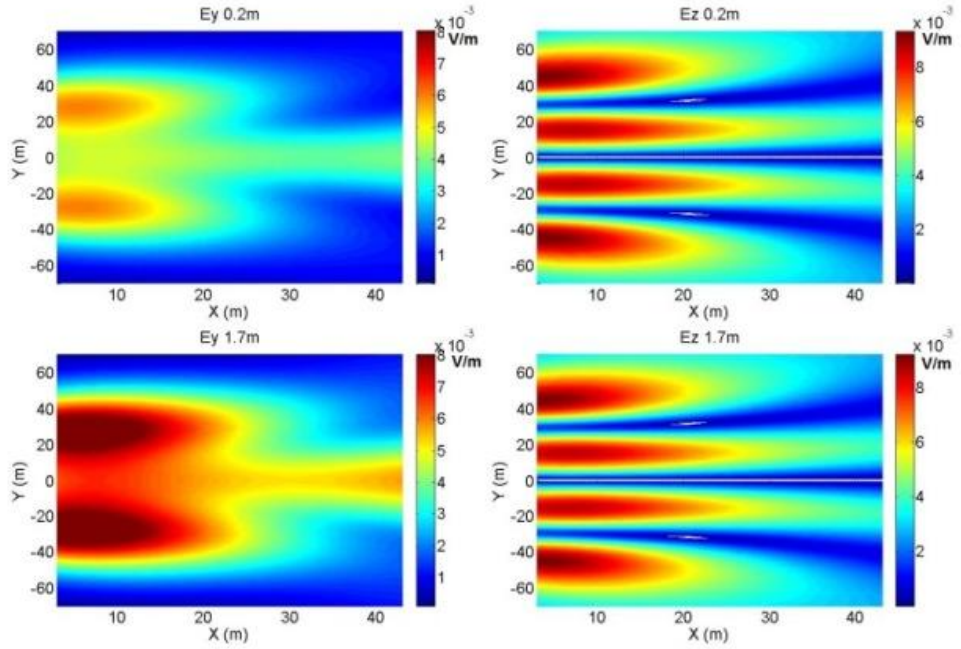

a) Near-field distributions calculated in NEC4

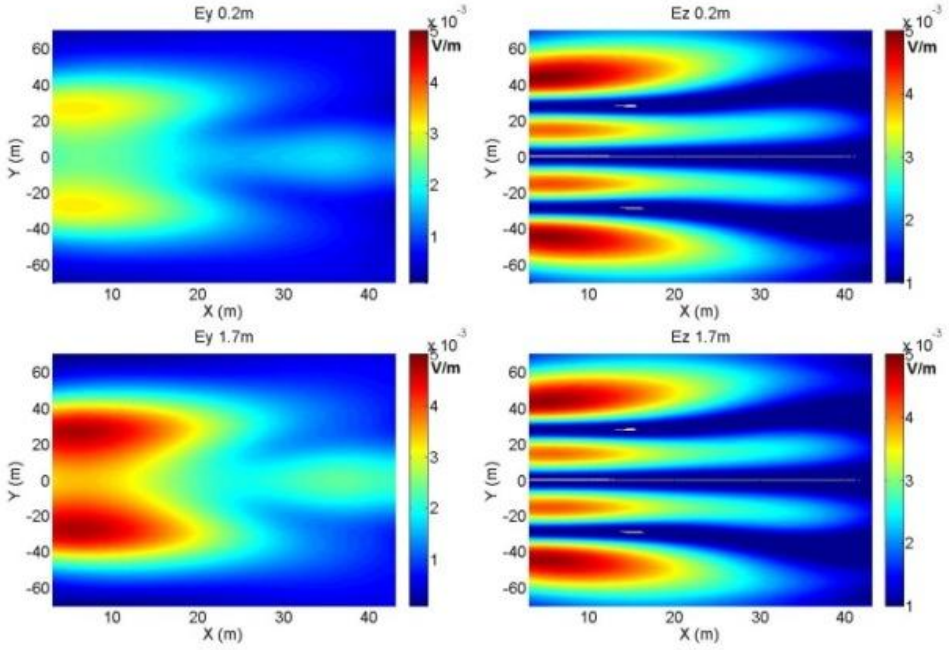

b) Near-field distributions calculated in CST

Fig 4.6 Array E-field without supporting towers above average lossy ground (1W).

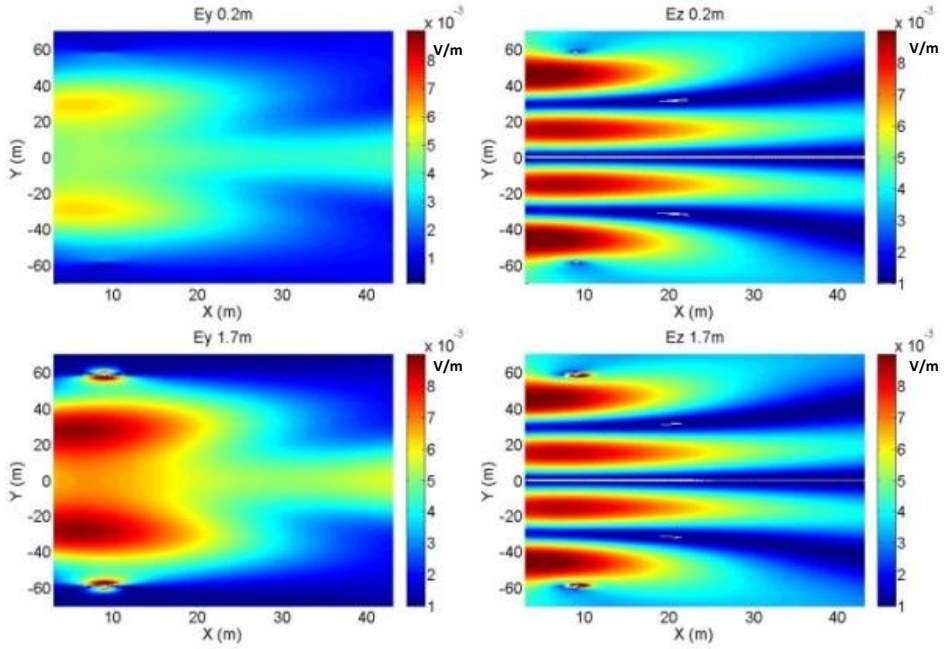

a) Near-field distributions calculated in NEC4

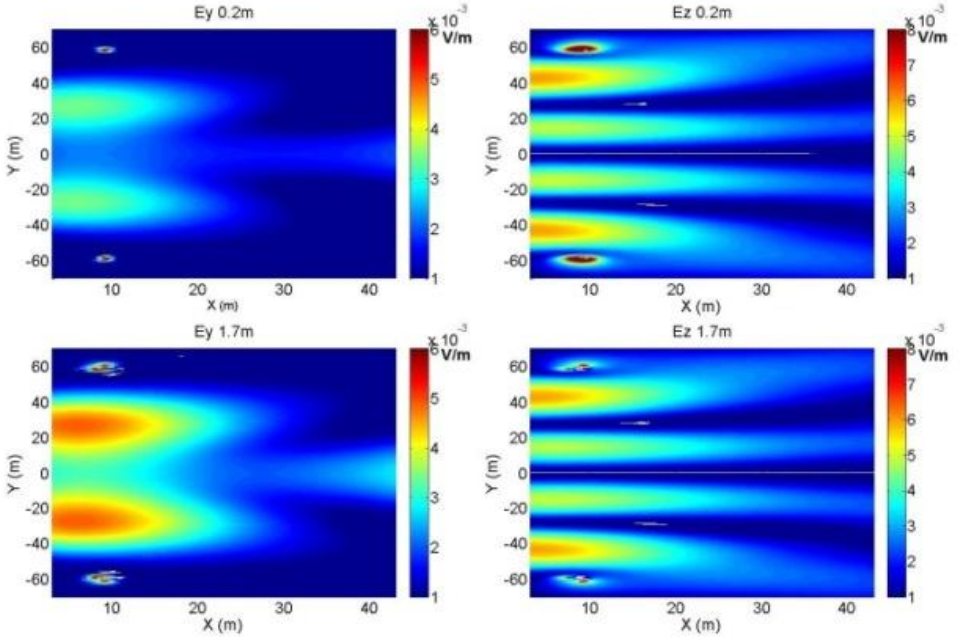

b) Near-field distributions calculated in CST.

Fig 4.11 Array E-field with supporting towers above average ground (1W).

Here a region up to approximately one wavelength in front of the array is the primary region of concern. The BBC world service HF curtain array (1W input power and 100% efficiency), with its support towers over different ground conditions has been modelled

and two numerical methods compared in Fig 4.8 to Fig 4.11. The results presented assist in mapping field distributions in the vicinity of high power HF transmission sites and can be used to assess both occupational and public exposure levels. Despite the curtain array consisting mainly of horizontal dipole elements the vertically polarized Ez component is shown to be strong within 20-25m in front of the centre of the array, irrespective of the ground type or the inclusion or exclusion of the supporting towers. The regions with the highest E-field values are shown to be in the regions where the towers are. However, the metal structured towers do not have a significant effect on the near-field distributions. It is still very important to notice that the modelling of the supporting towers is important when considering similar high power large scale modelling and the influence of their presence.

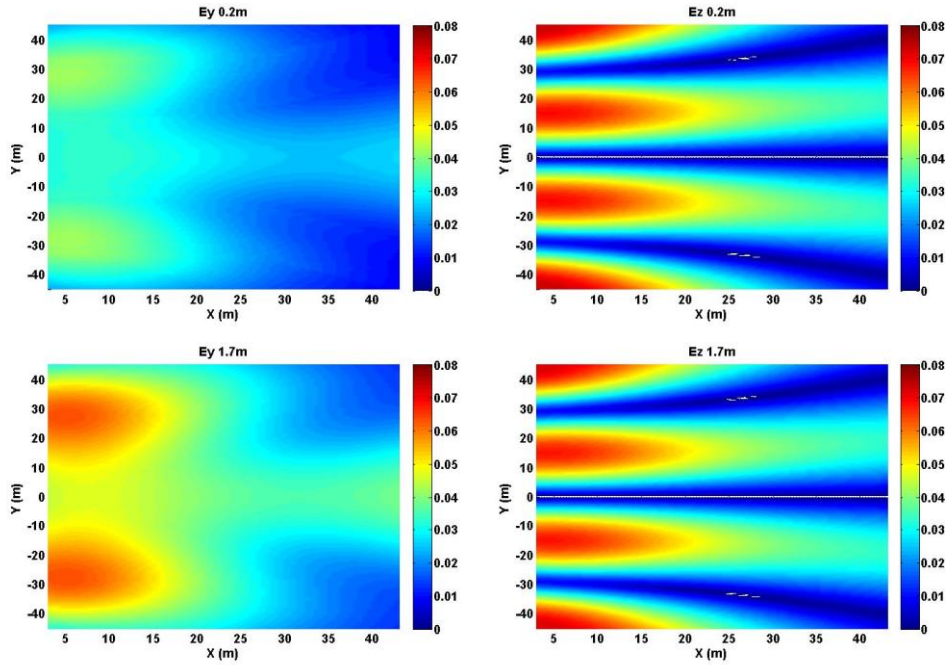

a) 1W near-field distributions calculated in NEC.

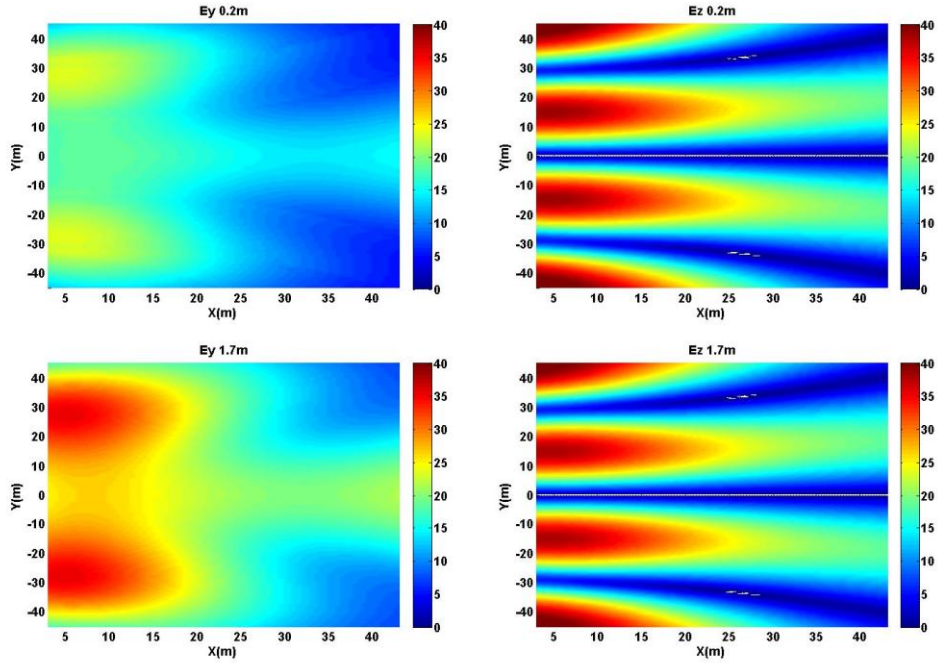

b) 300kW Near-field distributions calculated in NEC4.

Fig 4.7 Array E-field with supporting towers above average ground.

The towers do not have a significant influence, but the following simulations of models still included them. The region of interest for human exposure study purposes was deemed to be 45m from the center of the array and one-wavelength in front of the array. This is the area where the strongest EM appeared. Fig 4.12 compared the array at 1W and 300kW power radiation EMF field in the region of interest both above the AVG ground. Fig 4.13 and Fig 4.14 are 2-D Ey and Ez plots of 6m and 10m at different heights in front of the array at both power levels.

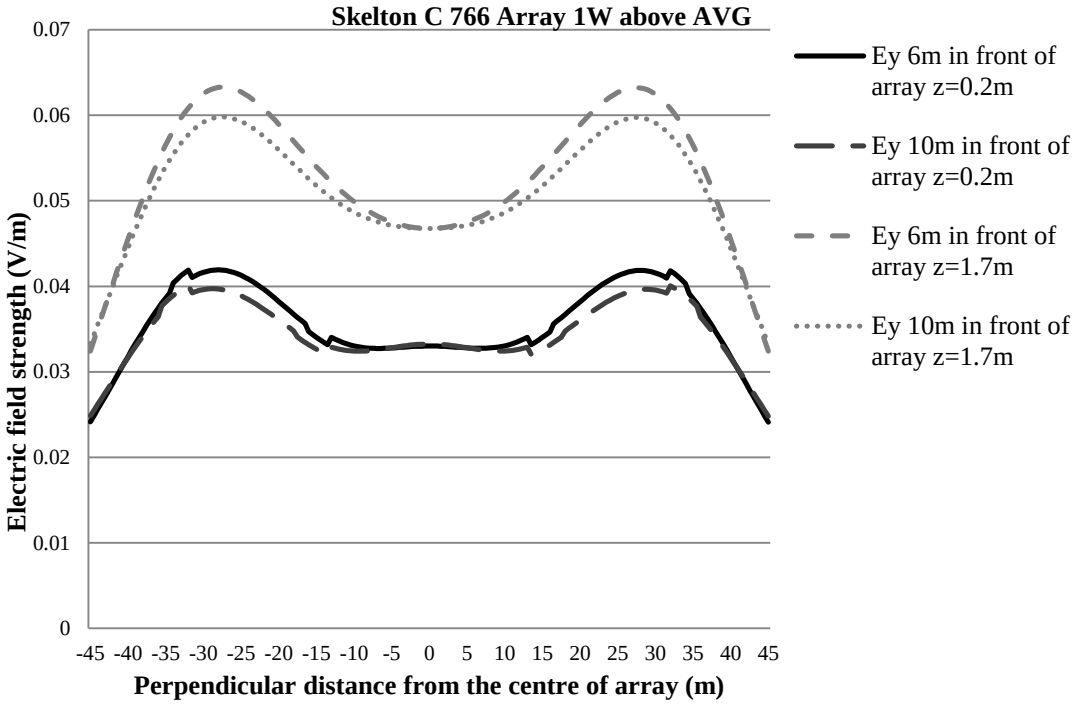

a) Ey

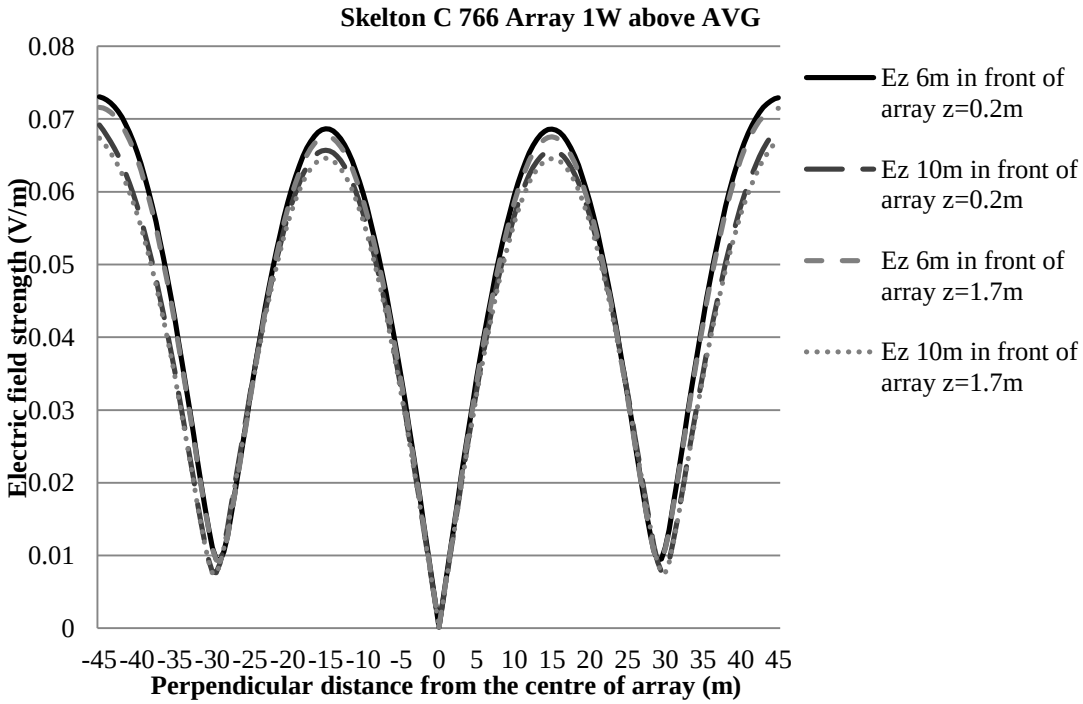

b) Ez

Fig 4.8 Skelton C HF curtain array 766 1W E-field in front of array.

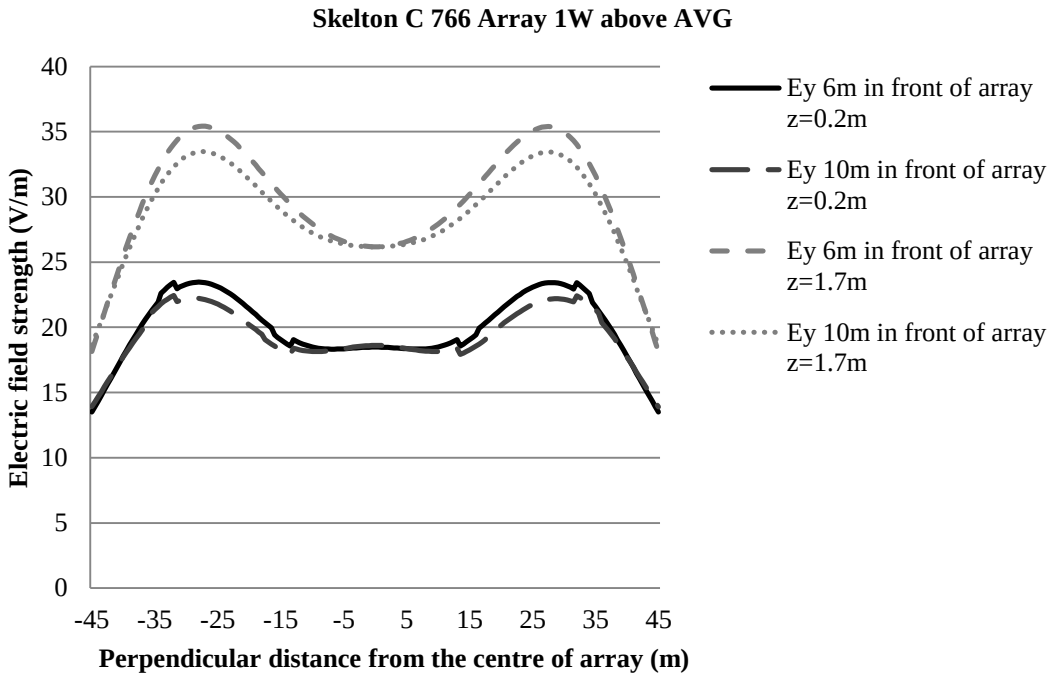

a) Ey

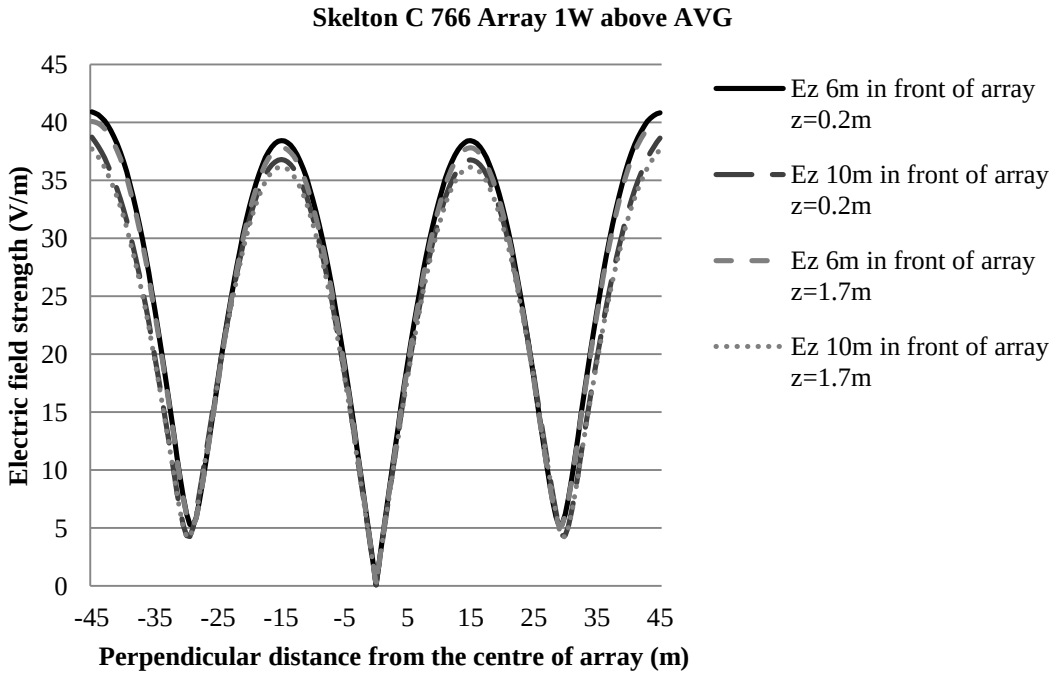

b) Ez

Fig 4.9 Skelton C HF curtain array 766 300kW E-field in front of array.

Horizontal E-field (Ey) values increase as the height increases; at shoulder height (at z = 1.7m) Ey is about 1.5 times higher than the value at the ankle height (at z = 0.2m). However, the vertical E-field has much less variation with height. The 300kW

powered antenna field strength is about 27dB higher than the 1W power antenna, which is the same as the increase in power in the near-field region of the antenna.

A summary of the peak E-field values of 1W input power models in NEC and CST microwave studio are shown below in Table 4.1. It can be seen that the results calculated using CST are consistently higher than those calculated in NEC.

NEC		Z(m)	Max (mV/m)	CST		Z(m)	Max (mV/m)
PEC	Ey	0.2	5.8	PEC	Ey	0.2	5.1
		1.7	49.4			1.7	58.2
	Ez	0.2	109.7		Ez	0.2	120.4
		1.7	109.5			1.7	120.1
AVG	Ey	0.2	5.8	AVG	Ey	0.2	61.9
		1.7	49.4			1.7	107.2
	Ez	0.2	109.7		Ez	0.2	33.0
		1.7	109.5			1.7	101.7

Table 4.1 Summary of peak E-field values in CST and NEC4 calculations at z=0.2 and 0.7 m, x=(0:43)m, y=(-45:45)m, in near-field region of array with its supporting towers model at 1W.

These results illustrate that there are high intensity E-field regions in front of the array for both vertical and horizontal components. Table 4.1 shows the peak field values and their locations for both horizontal and vertical components of the E-field in both numerical methods and ground conditions. Table 4.1 excludes the local area around both towers. These results appear asymmetrical due to the limitation of near-field point calculations and the subsequent quantisation errors. When using NEC4 a maximum of 66000 field points can be calculated for each simulation, and therefore a near-field sampling interval of 0.5m has been used within a 45x70m sized region. This region corresponds to 70m in the direction of propagation perpendicular to the array, and 90m (±45m) parallel to the array. For consistency a sampling interval of 0.5m was also used in CST, and values were calculated over the same region. Despite the asymmetry of the results in terms of the peak E-field value locations, both methods show a good level of agreement.

4.5 HF broadcasting transmission site ground environments

As the exposed human is within one wavelength of the high power, high gain broadcast antenna the effects of local terrain topography and ground infrastructure can be significant. For this reason the effects are thoroughly considered and analysed in this thesis.

4.5.1 Local terrain topography

A curtain array (6-7MHz) located at the Skelton C transmitting station in Cumbria, in the UK, has been used as the basis for this work. This particular array is built on a large unobstructed open grass field which has a slight (0.4 °) ground slope parallel to the face of the array. Ground (earth) conditions are considered as average ground having permittivity and conductivity values of $\varepsilon_r = 13$ and $\sigma = 0.005$ S/m. Simulations have been carried out at 6MHz and with a transmitter power of 300kW. All simulations included the the supporting towers located at either side of the array which is aligned along the y-axis at y=0m, with the antenna's main beam propagating along the x-axis.

4.5.2 Skelton C array ground slope modelling and simulation

The ground slope of Skelton C antenna site is discussed in this section. The modelling involved adding a tilting angle to the array and support towers in order to represent the ground slope. To compare the effects of the local terrain topography on the EMF, 8 models were built and re-simulated. Tilting angles up to 2 ° including 0.4 °, 0.5 °, 0.6 °, 0.7 °, 0.8 °, 0.9 °, 1.0 °, and 2.0 ° are considered. Table 4.2 compares the E-field values at 0 °, 0.5 °, 1.0 °, and 2.0 ° when the array was radiated at 300kW. The displayed points are 6m and 10m in front of the array at 4 different heights above the ground (0.2m, 0.5m, 1.7m and 2.0m), detailed results will be shown in Appendix B. Table 4.2 displays the changes of the field value; Fig 4.15 is the cut view of results (Table 4.2) location.

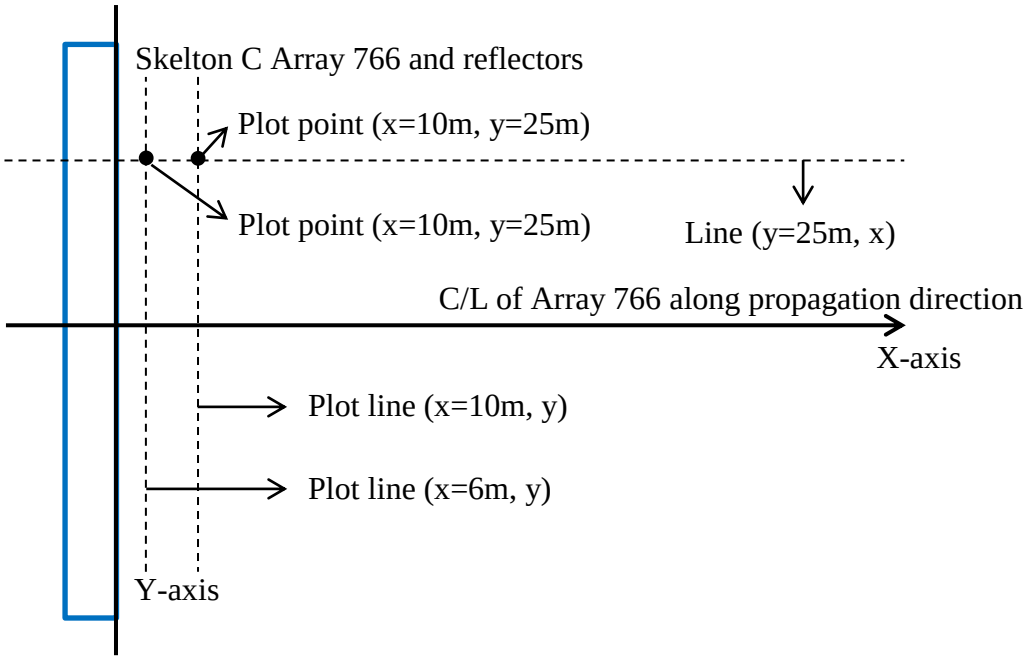

Fig 4.10 2-D field value plot geometry in accordance with the E-field distributions plot.

Y=25m*			**X=6 m****			**X=10m****		
Ground Slope (ϑ)			**0 °**	**1 °**	**2 °**	**0 °**	**1 °**	**2 °**
Height (m)	**0.2**	Ey	21.45	21.00	23.01	20.34	20.08	21.36
		Ez	20.99	22.00	30.89	21.08	21.88	30.73
	0.5	Ey	22.33	22.89	25.03	21.31	21.77	23.22
		Ez	14.33	15.15	20.12	14.35	15.08	20.05
	1.7	Ey	35.00	31.78	34.42	37.00	34.66	37.18
		Ez	20.04	21.97	30.18	19.12	21.84	29.83
	2.0	Ey	30.93	28.92	31.74	32.74	31.51	34.38
		Ez	13.73	14.94	19.22	13.22	14.87	19.00

Table 4.2 Ground slope E-field variations (array powered at 300kW) above AVG.

*Array aligns with data plot y-axis.
**Propagation direction aligns with x-axis

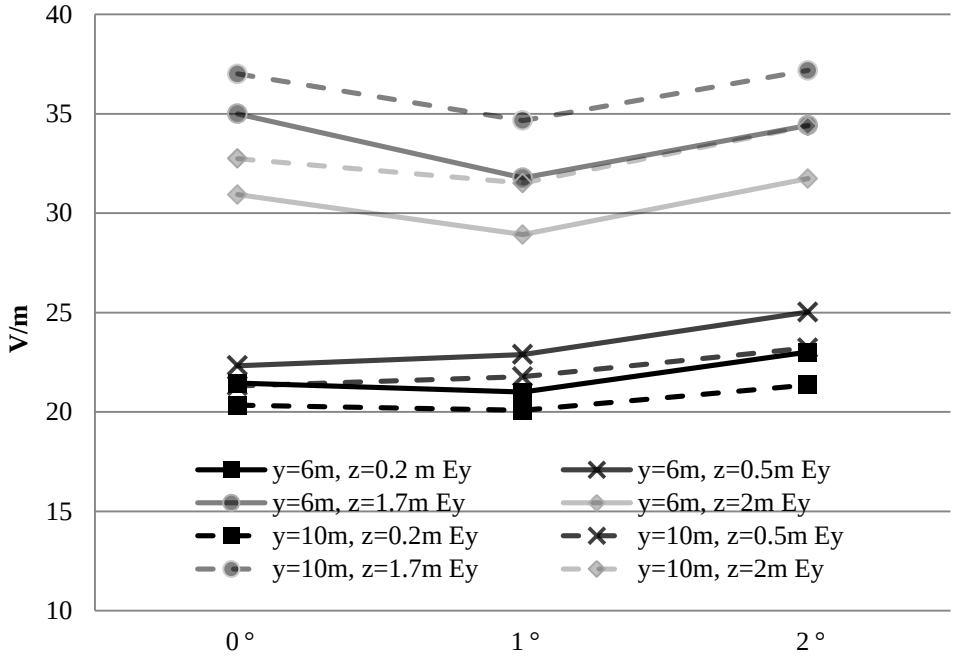

a) Ey

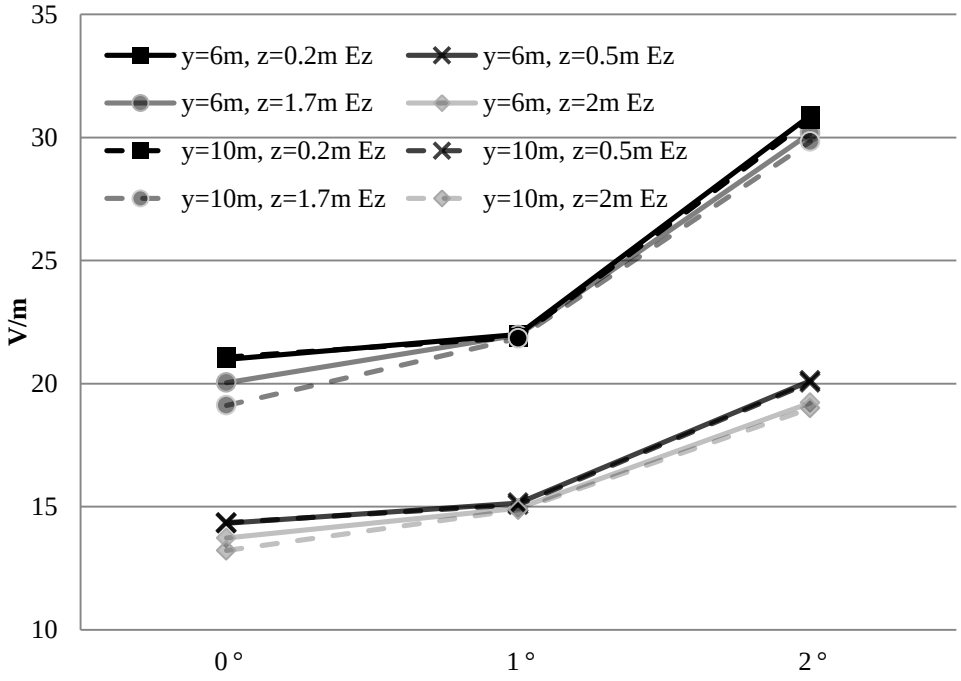

b) Ez

Fig 4.11 Comparison of horizontal Ey and vertical Ez with 0 °, 1 °, 2 °ground slope at y=25m and x=6 and 10m in front of array when 0.2m and 1.7m above the ground.

As shown in Fig 4.16 the ground slope has more effect on the horizontally polarized E-field than the vertical E-field. The strength of Ey increases as the height is increased until 1.7m above the ground. But at 2m height above the ground the Ey strength level dropped below the Ey value at 1.7m high. At 1.7m to 2.0m height, when the flat ground is increased to a 1 ° ground slope, Ey has a 2-3 V/m drop from 1.7m to 2m. When the slope continues to rise to 2 °, the field value increases back to almost the same as for the flat ground condition. For the vertically polarized E-field, the strength only increases as the ground slope angle increases. From flat ground to 1 ° slope the value of Ez increases by 2-3V/m but jumps as high as 10 V/m when the ground slope increases to 2 ° from 1 °.

4.5.3 Array infrastructure

The effects of different levels of antenna structure complexity are also considered, along with variations in ground topology. Photos of the Skelton HF curtain array 766 including the supporting towers and feed network are shown in Fig 4.1. The two supporting towers are approximately 90m tall and the centres of the towers are approximately 135m apart. Directly beneath the array is the main antenna feed, power dividers, matching networks, feeds to the radiating elements and structural tension wires. All the wires, poles and tubes are exposed to the air without dielectric coatings. The ground feed networks are all supported and lifted approximately 4m above the ground by 8cm diameter hollow metal poles.

Models based on the original construction plans were produced for increasing levels of complexity of the antenna structure. Fig 4.17a shows the array and two supporting towers on both sides without infrastructure beneath. The addition of just the vertical poles, which are 4m tall (~λ/12) and normally support the main feed, and splitters are shown in Fig 4.17b. Fig 4.17c shows the inclusion of the 30m long element feeds and the ground level tension wires. Fig 4.17d shows the lower section of one of the element feeds with the addition of a balun and splitter support box tower, while Fig 4.17e shows the full feeder network, tension wires and towers.

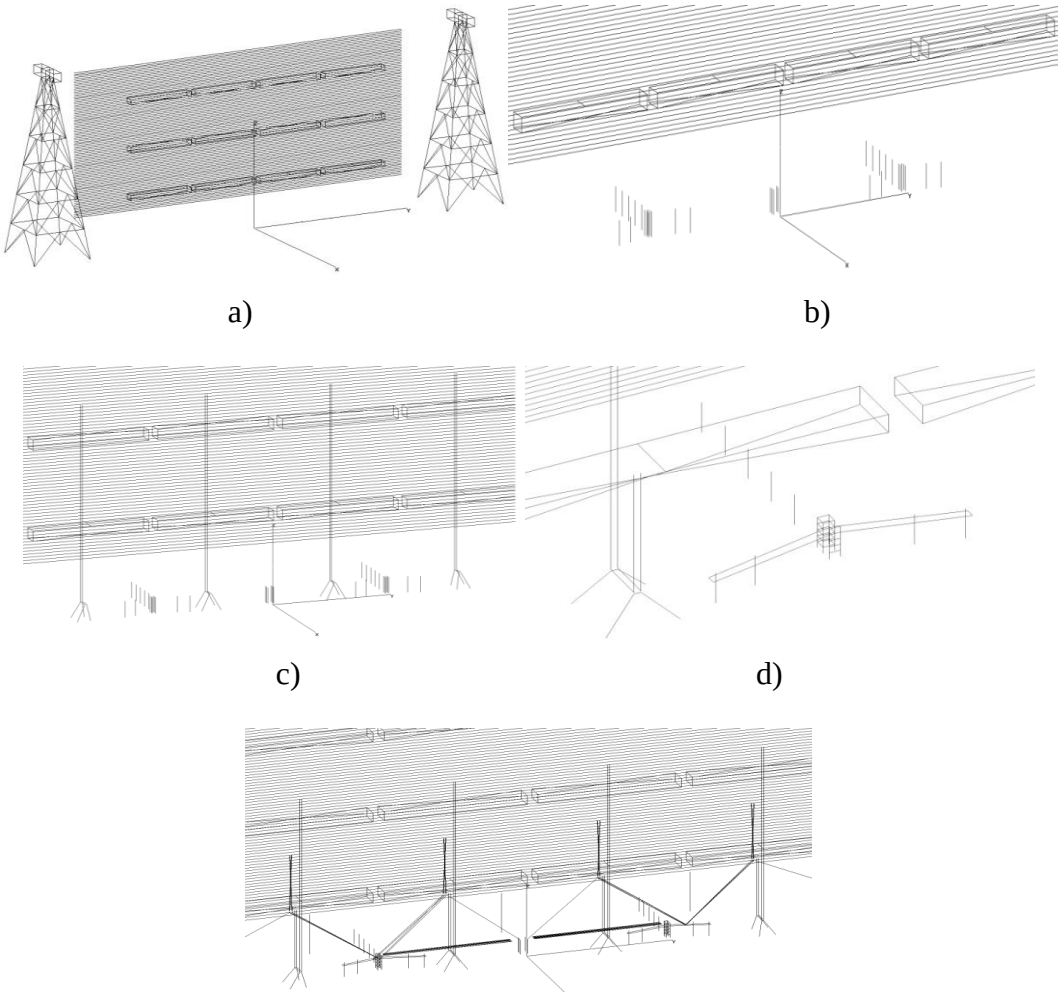

Fig 4.17 Antenna infrastructure models above a perfectly flat average ground: a) basic model, and with addition of b) vertical support poles, c) element feeder connections, d) splitter supporting box tower and balun, e) full feeder network, tension wires and towers (not shown).

Simulations were performed to assess how increasing the antenna structure complexity alters the horizontal (Ey) and vertical (Ez) electromagnetic field strength values within the near-field. Fig 4.18 shows comparisons between simualted near vertically and horizontally poloarized E-field distributions in front of the array with various feeder bay structures at a height of 1.7 m above a perfectly flat average ground. The field distribution plots in Fig 4.18a-e correspond to the configurations shown in Fig 4.17a-e.

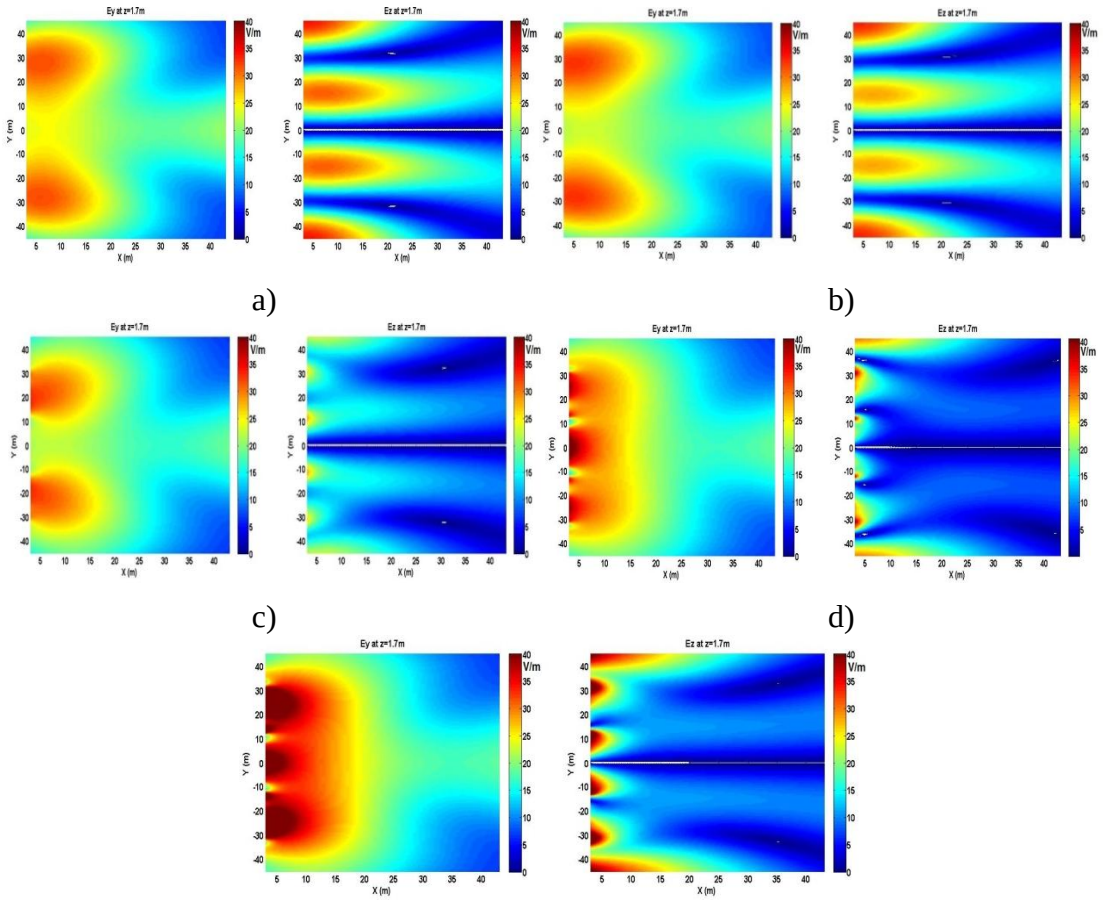

Fig 4.12 Comparison between horizontal (Ey) and vertical (Ez) E-fields in front of the array at height of 1.7 m above a perfectly flat average ground at 250KW [4.9]. a) basic model, and with addition of b) vertical support poles, c) element feeder connections, d) splitter supporting box tower and balun, e) full feeder network, tension wires and towers.

Fig 4.17a-c showed the ground vertical metal structures that were modelled. The field distributions were plotted accordingly in Fig 4.18a-c, it can be clearly seen that the horizontal E-field was significantly reduced while the horizontal E-field was less affected. When horizontal metal wires were introduced in the models (Fig 4.17d-e), the Ey field in the region very close to and right in front of and underneath the array was noticeably altered as shown in Fig 4.18d-e. Compared with only vertical metal structures, the horizontal metal structures intensified the Ey in the near-field within a 20m range. The vertical E-field (Ez) also increased. Fig 4.18 demonstrated these structures underneath the array significantly affected the field distributions. The incident wave $E^i(r)$ of the antenna impinges on the wire or poles which produce an induced current and turn these structures into scatterers. They produced a new electric field, referred to as the scattered electric field $E^s(r)$. By applying Pocklington's

Integral Equation, then the total electric field $E^t(r)$ is sum of both incident and scattered field [4.10].

$$E^t(r) = E^i(r) + E^s(r) \quad (4.1)$$

Where

$E^t(r)$ = total electric field

$E^i(r)$ = incident electric field

$E^s(r)$ = scattered electric field

Although the supporting structures were assembled by fragments, some of them are still over 8m long very close to the antenna. Because the broadcast antenna operates at such high power, its incident field levels are high, resulting in high induced current in those structures. These wire or poles are not only good scatterers but could also be seen as vertical monopole antennas and horizontal dipoles. A monopole antenna is known as one half of a vertical dipole antenna. The electric components of the radiated energy are parallel to the polarization of the dipole. Therefore, depending on these structure's locations and length, these scattered fields could cancel or enhance the vertical and horizontal E-field components. These structures significantly changed the near-field of the antenna. The near-field distribution and levels become very complex. As introduced in Chapter 2, the ICNIRP only give specified basic restrictions and reference level by the frequency range. The environment humans are exposed to varies. These structures and their influence to the field distributions are essential to assess the human exposure in the near field of HF antennas. These can be applied to similar HF broadcast transmitters or RF exposure problems.

Besides variation in the antenna ground infrastructures, the ground conditions where the transmitters are built also vary from place to place. As explained earlier in this chapter, for HF communications the antennas are arrays of centre fed simple horizontal half-wave dipoles. They are relatively simple wire antennas and it may be easily studied by applying theoretical performance analyses. These also have been proven in practice. However, most of the analyses were for broadcasting radio including communication efficiency, radiation patterns, gain or directivity, VSWR and power handling capability. HF radio waves transmit via reflection from the earth F^2-layer

ionosphere. The ground is also a reflector. For simplicity the ground normally was considered flat and perfect conducting. However, the actual ground is lossy; it reflects part of the radio frequency energy and also absorbs some. The ground related factors might not be significant for HF communications, but they need to be taken into account when evaluating the near-field of antennas. Therefore, after ground infrastructure was added, the ground slope and its effects were studied. A ground slope was also added to the Skelton C HF curtain array 766 model. The full transmission array models are as displayed in Fig 4.19:

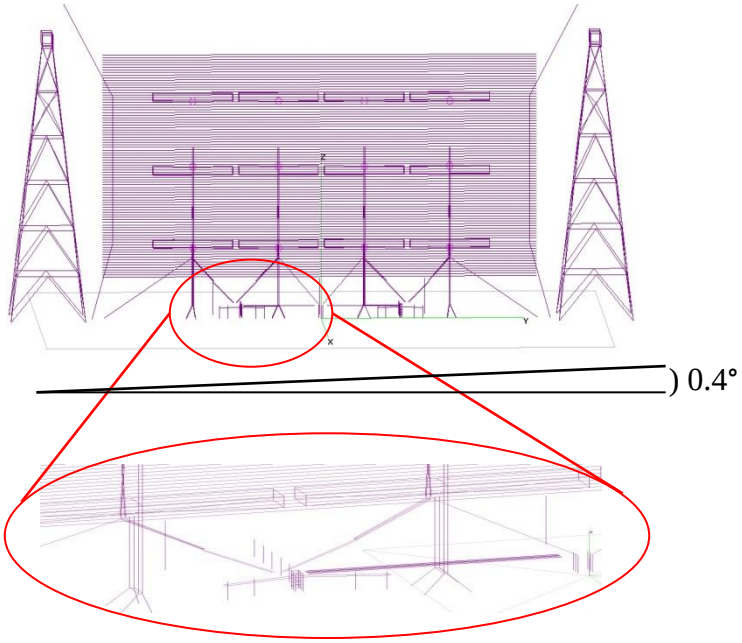

Fig 4.19 Skelton C HF curtain array and its infrastructure with ground slope.

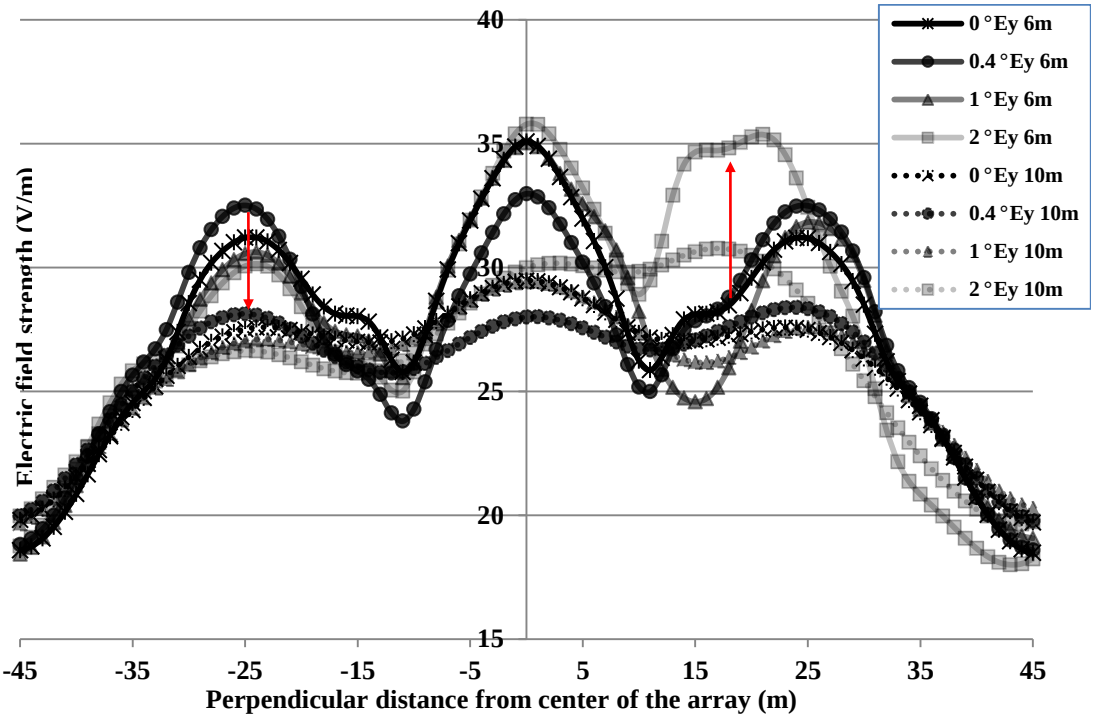

Fig 4.13 Horizontaly polarized E-field 6m and 10m in front of the HF curtain array tilted at various angles, Z= 1.7m.

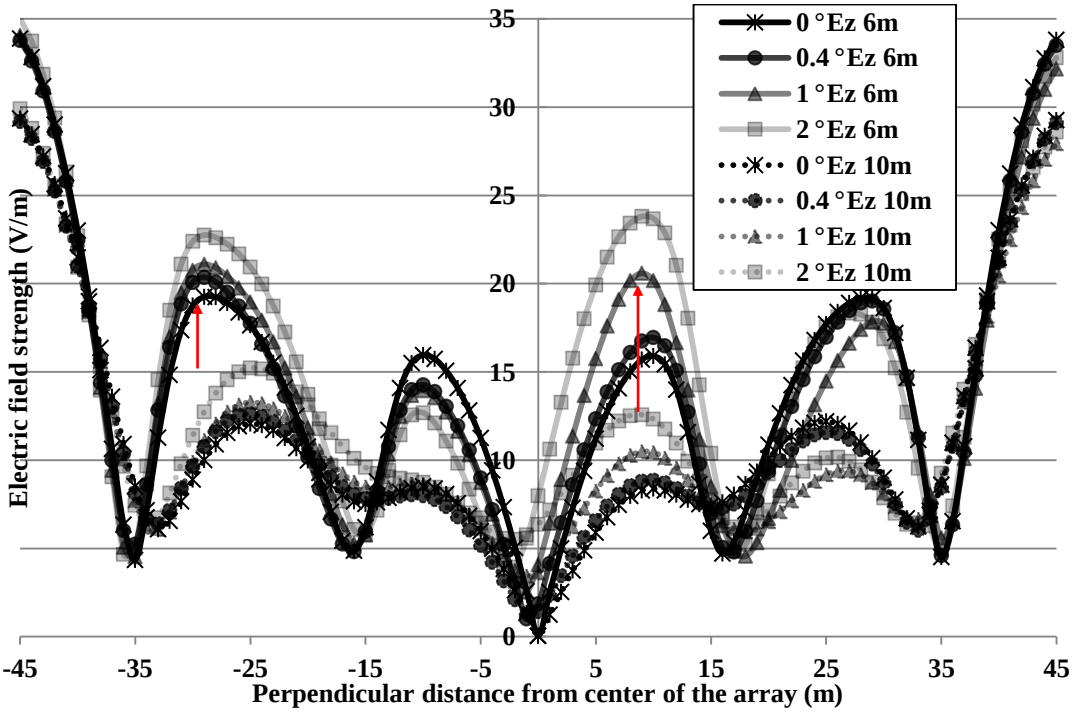

Fig 4.14 Vertically polarized E-field 6m and 10m in front of the HF curtain array tilted at various angles, Z= 1.7m.

The effects of the local terrain topology on the near-field distributions have been studied by varying the slope of the ground relative to the array. An illustration of the

model including the supporting towers, feed network, and ground slope is shown above in Fig 4.19. Results are shown comparing samples taken at 6m and 10m in front of the array for different ground slope angles. To represent the ground slope the entire model (array, feed structure and supporting towers) was tilted at 0°, 0.4°, 1° and 2°. The resulting horizontal (Ey) and vertical (Ez) E-field components are shown in Fig 4.20 and Fig 4.21 respectively. The E-fields were sampled at 1m intervals and at 1.7m height above the ground corresponding to the shoulder height of an average male adult.

It can be seen that for both the horizontally and vertically polarized E-fields, the ground slope caused asymmetry in the field distribution and that the electric field strength increases as the ground slope increases. The change in ground slope affects the E-field components differently. For the horizontally polarized case (Fig 4.20), when compared to a perfectly flat ground, a 2° ground slope increases the electric field strength 6m in front of the antenna array by approximately 7V/m at a location 20m from the centre of the array and reduces the electric field strength by 3V/m at a location -25m from the centre of the array. For the vertically polarized case (Fig 4.21) the same increase in ground slope results in an increase of electric field strength of 8V/m and 4V/m at a distance 6m in front of the antenna array, at locations 10m and -30m from the array's centre.

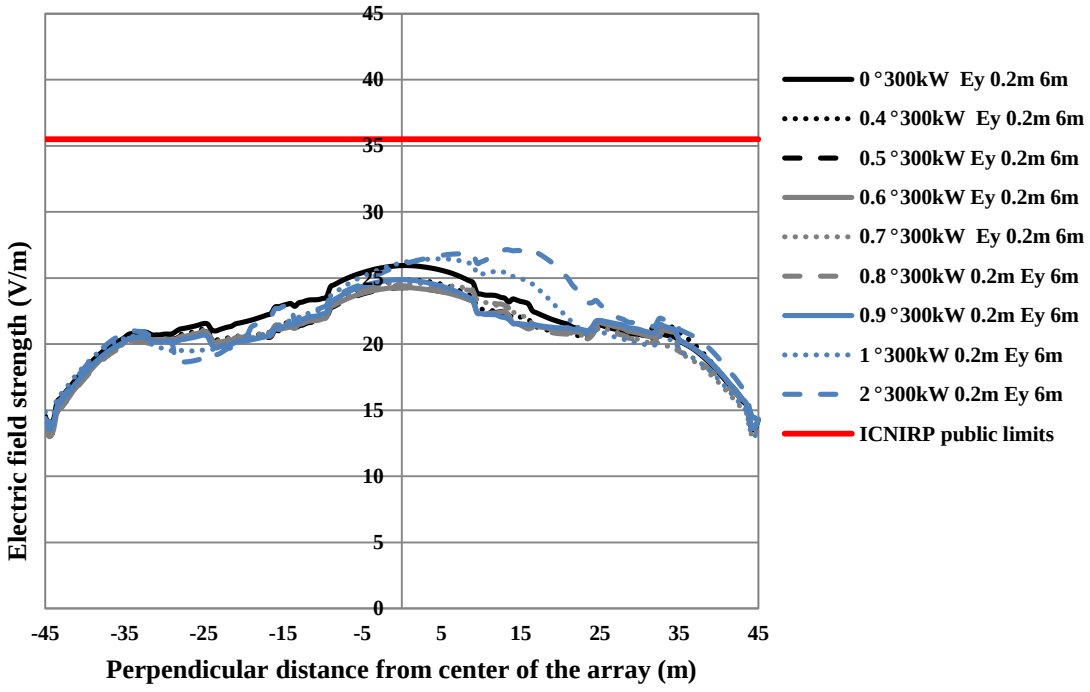

a) 300kW Ey at z=0.2m 6m in front of the centre of array.

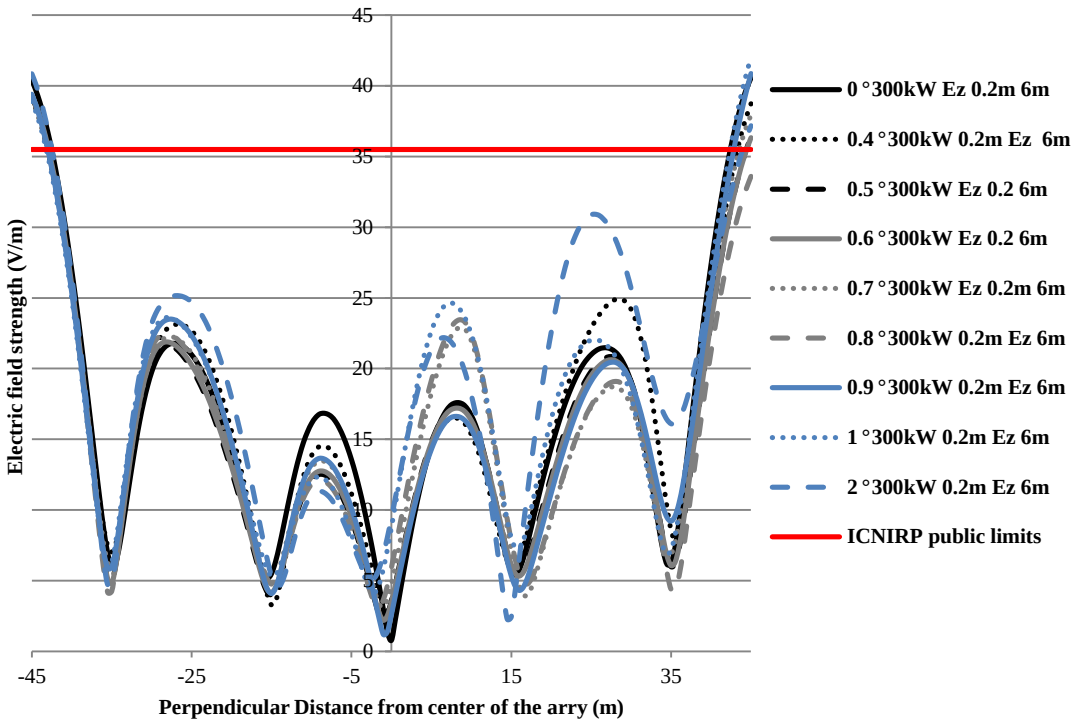

b) 300kW Ez at z=0.2m 6m in front of the centre of array.
Fig 4.15 Field line plot in front of array.

Plots of Ey (Fig 4.22a) and Ez (Fig 4.22b) compared 6m in front of array at 300 kW power between the ground angle increased from flat to 2 °. The red line is the ICNIRP recommended limits for public exposure (35.5 V/m).

4.5.4 Power comparison

In previous section of this chapter, there were comparisons between 1W and 300kW powered simple array models, without considering the local terrain topography and array infrastructure. BBC Skelton C HF broadcasting array 766 operates 6-7 MHz radio at 300kW. Other HF transmitting antennas operate up to 500kW such as Cyprus Zygi transmission site for BBC World Service or Greenville for Voice of America (VoA). In the previous section of this chapter, an increase in the model's power level from 1W to 300kW proportionally increased the field strength level in the near-field region. This section looks into the effects of increased power levels along with an increase in ground slope angle on the full model (Fig 4.19). Fig 4.23 and Fig 4.24 show the comparison of the full model irradiating at 200kW, 250kW and 300kW with ground angles 0 °, 0.7 ° and 2 °.

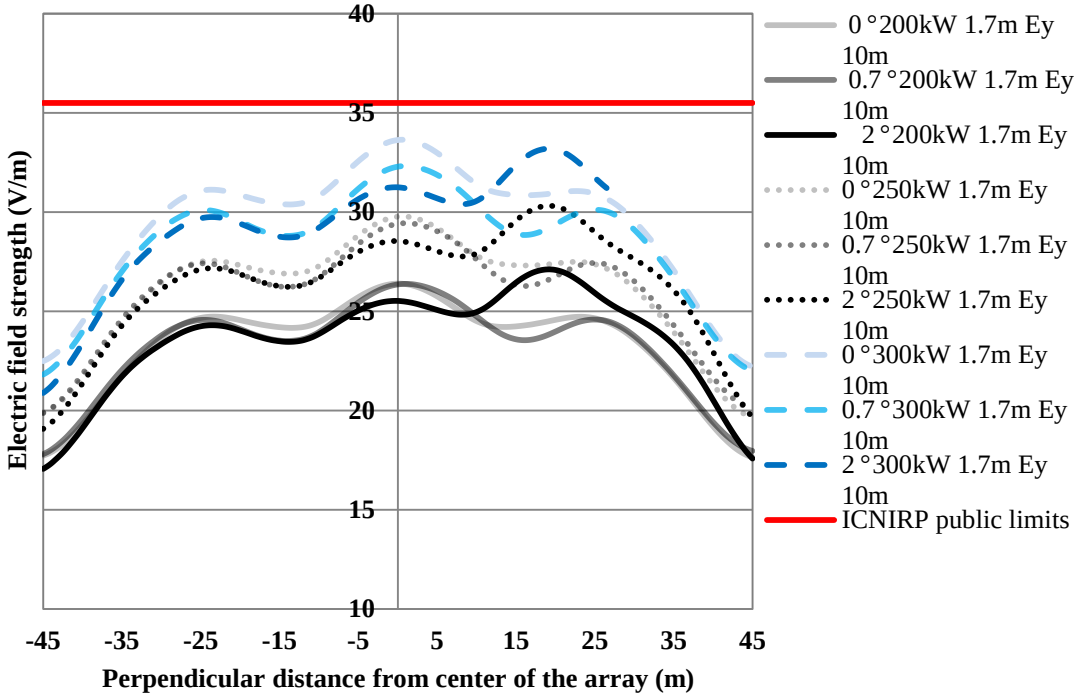

Fig 4.16 Power Comparison Ey at z=1.7m 10 m in front of the centre of array.

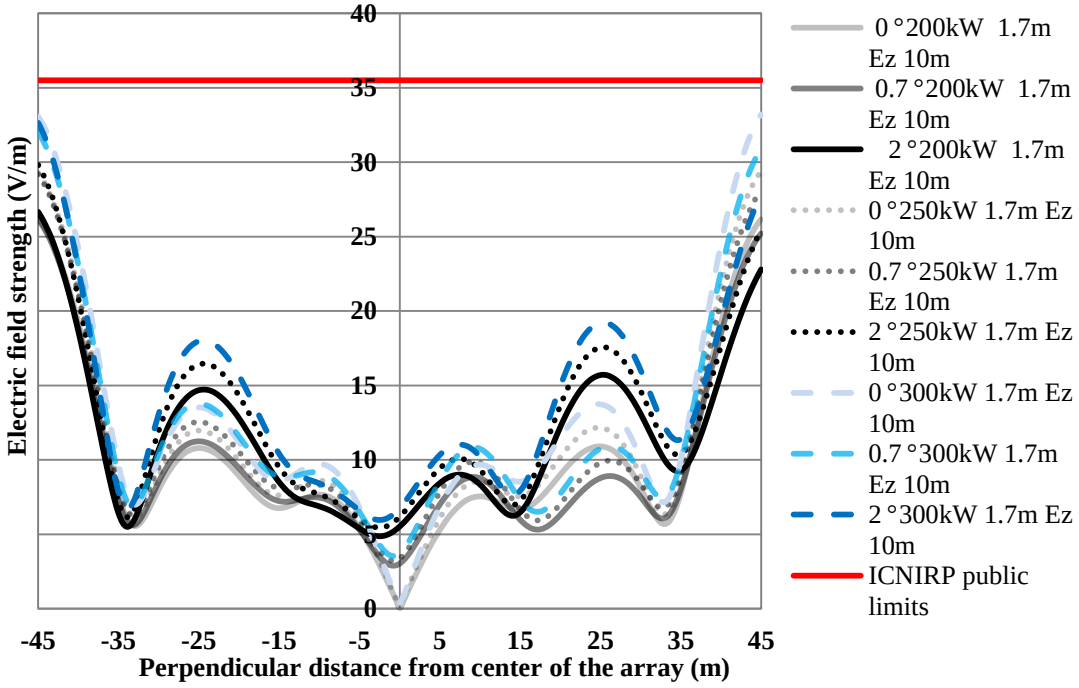

Fig 4.17 Power Comparison Ez at z=1.7m 10 m in front of the centre of array.

The red line in Fig 4.21 and 4.22 indicated a 35.5V/m ICNIRP public exposure limits while occupational exposure limits are 101.7 V/m.

Fig 4.25 and 4.26 compare the maximum horizontal and vertical E-field strength at 0.2m and 1.7m above the ground. The samples were taken at 6m and 10m in front of

the array along the propagation direction. At these distances, which are normally applied with occupational exposure limits, the maximum E-field strength value is still below the ICNIRP public exposure restrictions level. Table 4.3 shows the maximum E-field values in both polarizations at 200 kW, 250kW, and 300kW when the ground slope angle was at 0 °, 0.7 ° and 2 °. Fig 4.24 compares the maximum horizontal Ey and Ez at various ground angles.

Ground angle	Power /kW	0 °				0.7 °				2 °			
Polarization		Ey		Ez		Ey		Ez		Ey		Ez	
In front of array/m		6m	10m	6m	10m	6m	10m	6m	10m	6m	10m	6m	10m
Maximum E-field z@0.2m	200	20.44	18.73	32.07	27.56	20.13	18.47	31.97	27.41	22.16	19.81	33.37	27.88
	250	22.97	21.00	35.90	30.84	22.46	20.61	35.68	30.59	24.78	22.15	37.31	31.18
	300	25.95	23.26	40.56	34.84	20.78	22.63	39.17	33.58	27.14	24.25	40.86	34.13
Maximum E-field z@1.7m	200	31.42	26.40	30.29	26.24	31.36	26.38	30.28	26.16	32.81	27.11	31.70	26.66
	250	35.52	29.78	34.01	29.39	35.00	29.44	33.79	29.19	36.69	30.32	35.45	29.81
	300	40.13	33.645	38.43	33.20	29.794	32.33	37.10	32.05	40.17	33.20	38.81	32.64

Table 4.3 Maximum E-field (V/m) with varied Input Power and ground slope.

Maximum Ey and Ez in various ground slope simulations highlighted in Red

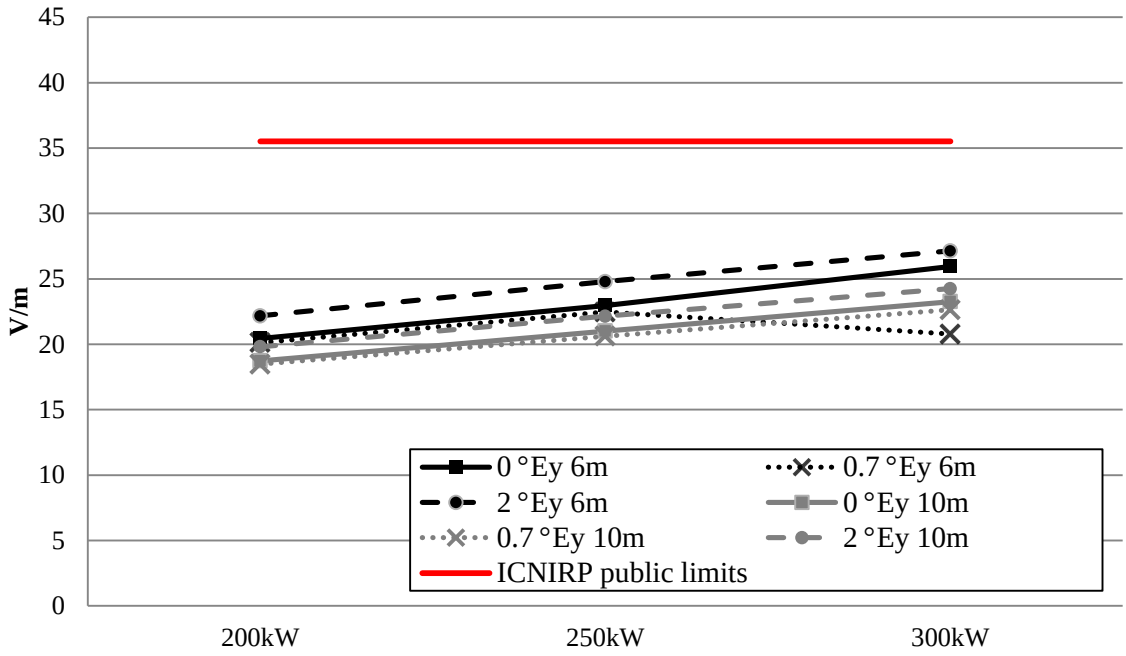

a) Maximum Ey in z=0.2m

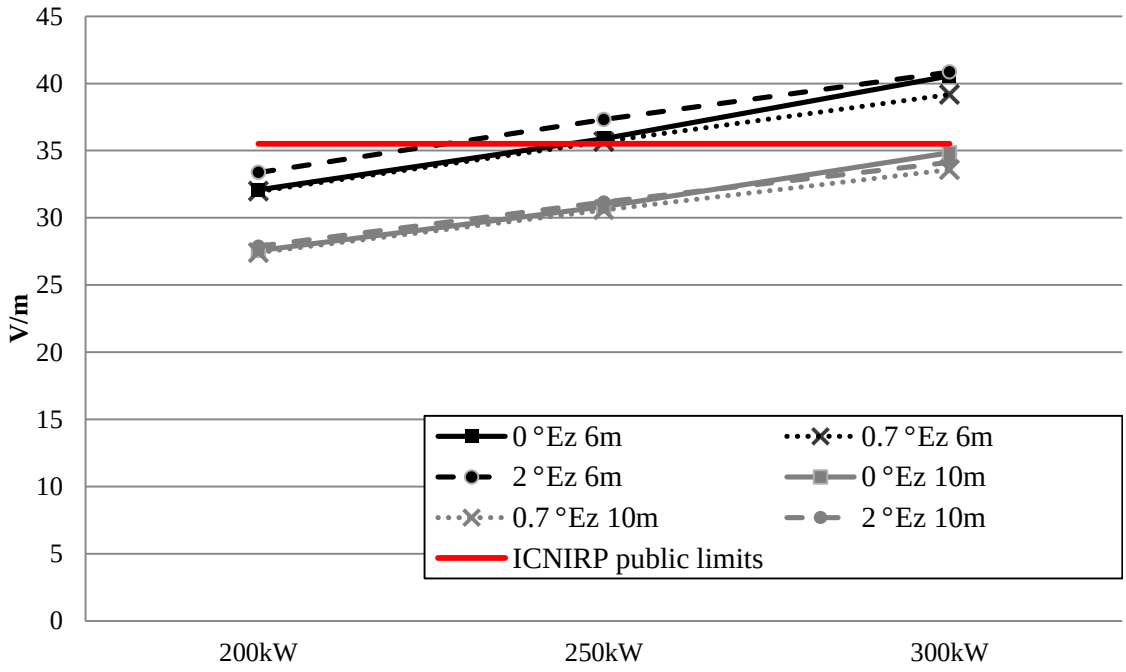

b) Maximum Ez in z=0.2m

Fig 4.18 Maximum horizontal Ey and vertical Ez comparison when 0 °, 0.7 °, 2 °ground slope occurs at 0.2m above the ground.

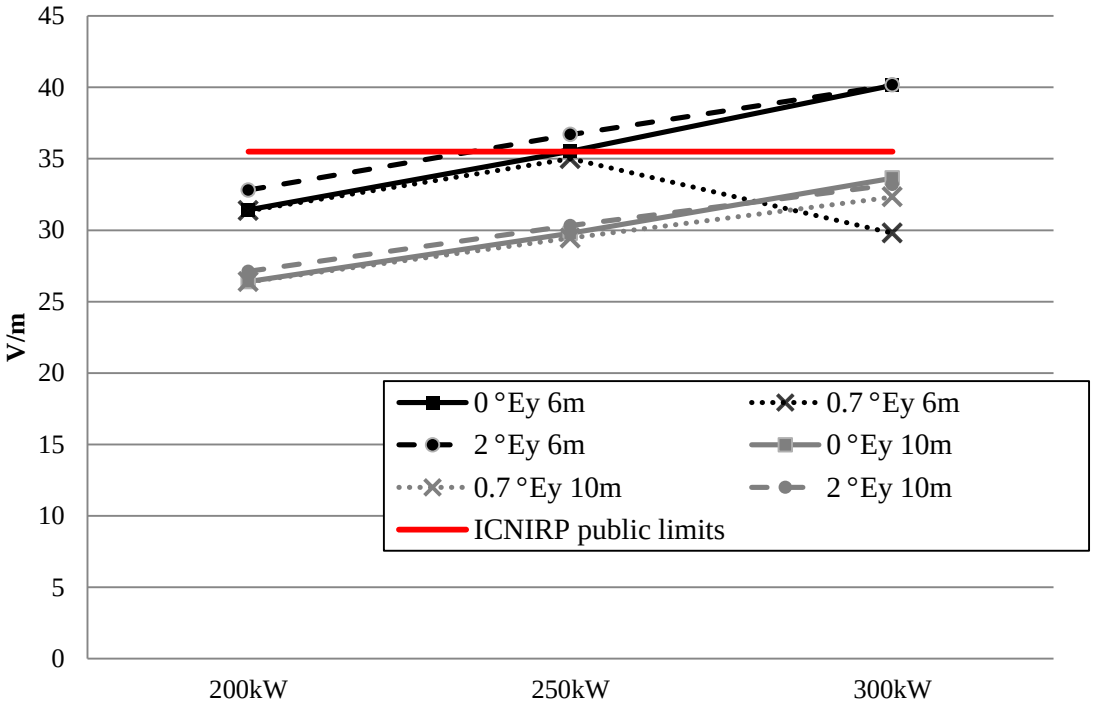

a) Maximum Ey in z=1.7m

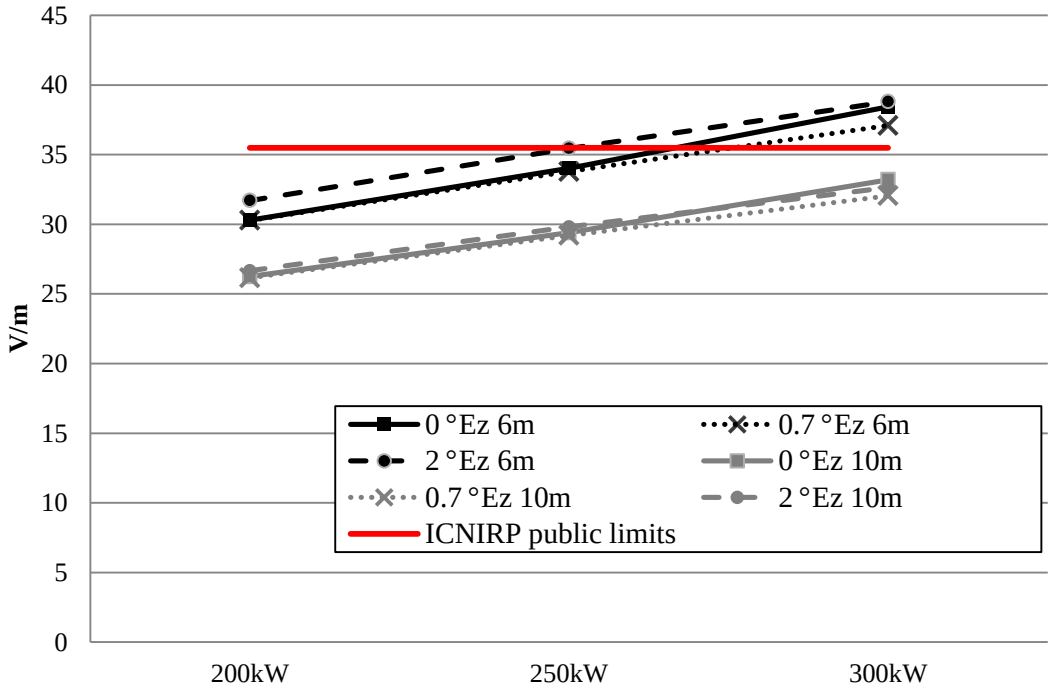

b) Maximum Ez in z=1.7m

Fig 4.19 Maximum horizontal Ey and vertical Ez comparison when 0 °, 0.7 °, 2 °ground slope occurs at 1.7m above the ground.

4.5.5 Summary of high power full Skelton C curtain array antenna 766 field distributions over different ground conditions

This section summarises the near-field EMF distribution for a full scale antenna model, including self-supporting towers, array infrastructure and ground slope. The EMF field distributions are mapped in Fig 4.27 - Fig 4.29. The dielectric properties of the ground have significant effects on the near-field of the array. 0.2m, 0.5m, 1.7m and 2.0m height z planes are all mapped and compared. These results included all previous investigated aspects of influential factors. Fig 4.27 shows the EMF of the full Skelton C transmission site on a flat ground above a PEC ground, while Fig 4.28 is simulated above a realistic average ground condition. Fig 4.29 shows the EMF distribution of the full scale model over an AVG with 2 ° ground slope. The effects of radiation power, ground conditions and ground slope are shown clearly in these E-field distribution plots.

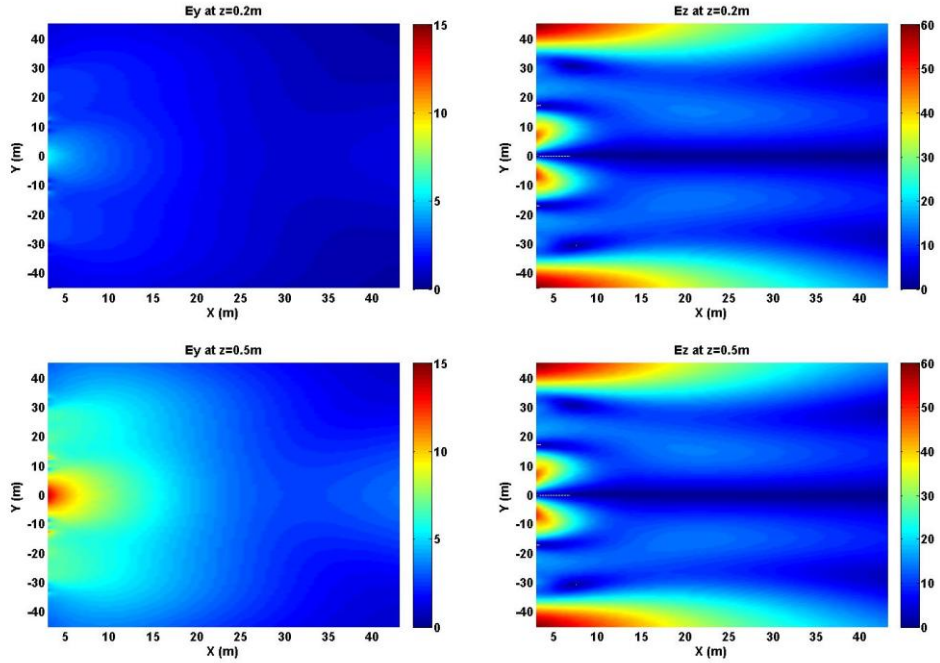

a) Height 0.2m and 0.5m above the ground

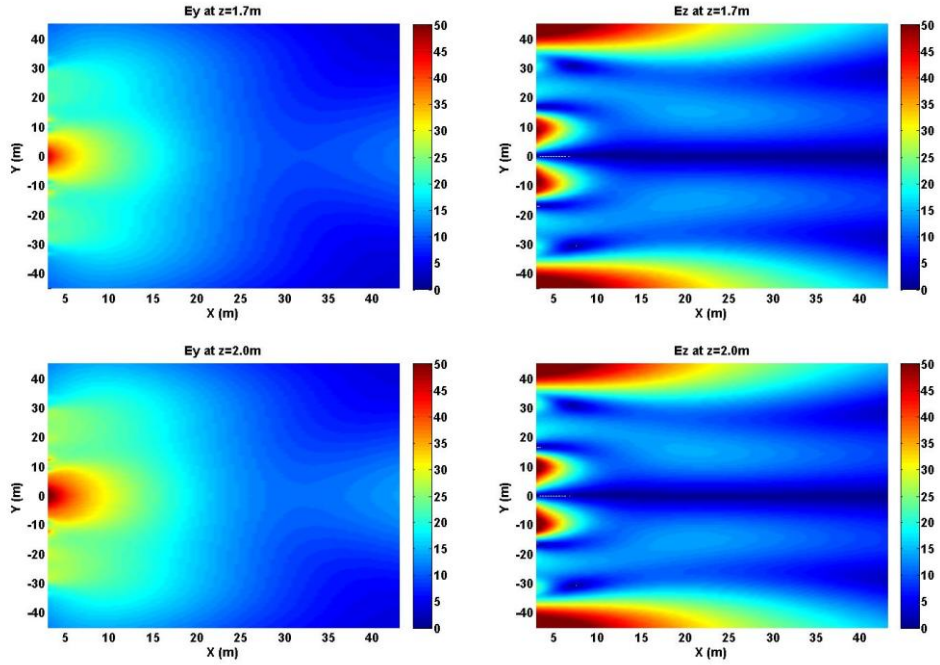

b) Height 1.7m and 2.0 m above the ground

Fig 4.27 Full model with 0 °ground slope 300kW power over PEC.

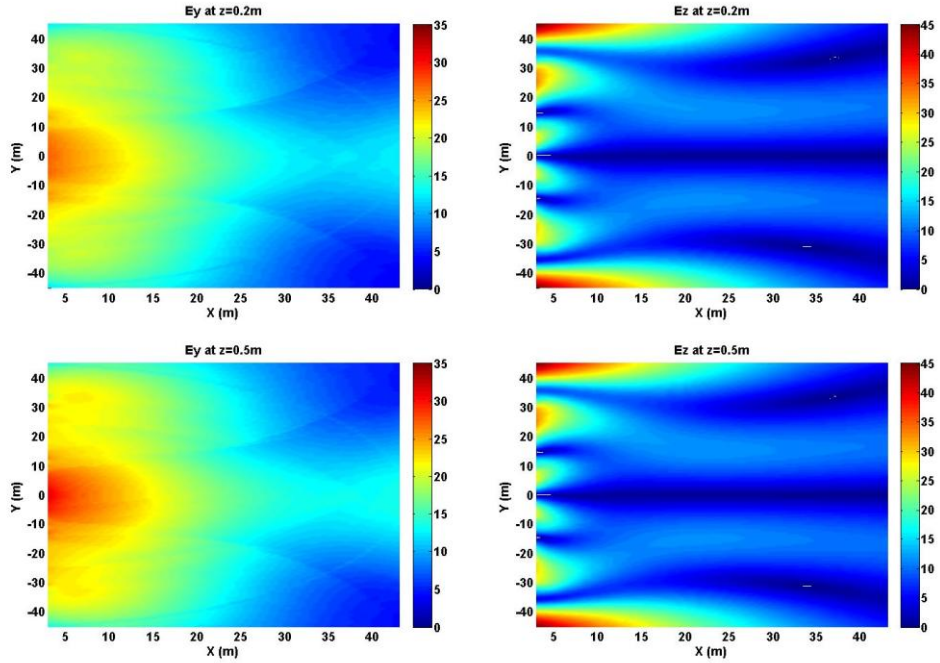

a) Height 0.2m and 0.5m above the ground

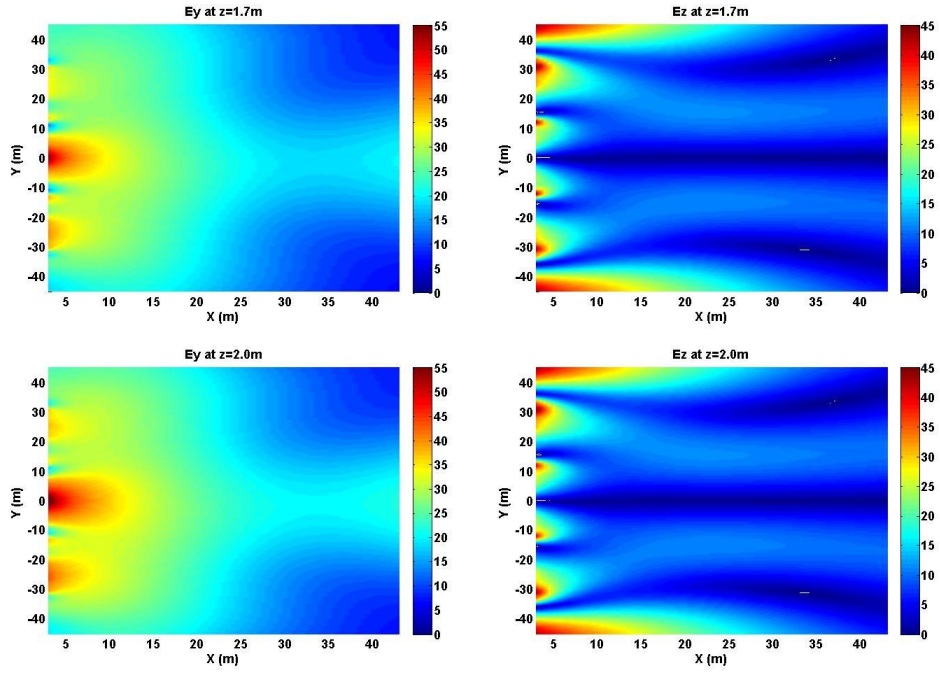

b) Height 1.7m and 2.0m above the ground

Fig 4.28 Full model with 0 °ground slope 300kW power over AVG.

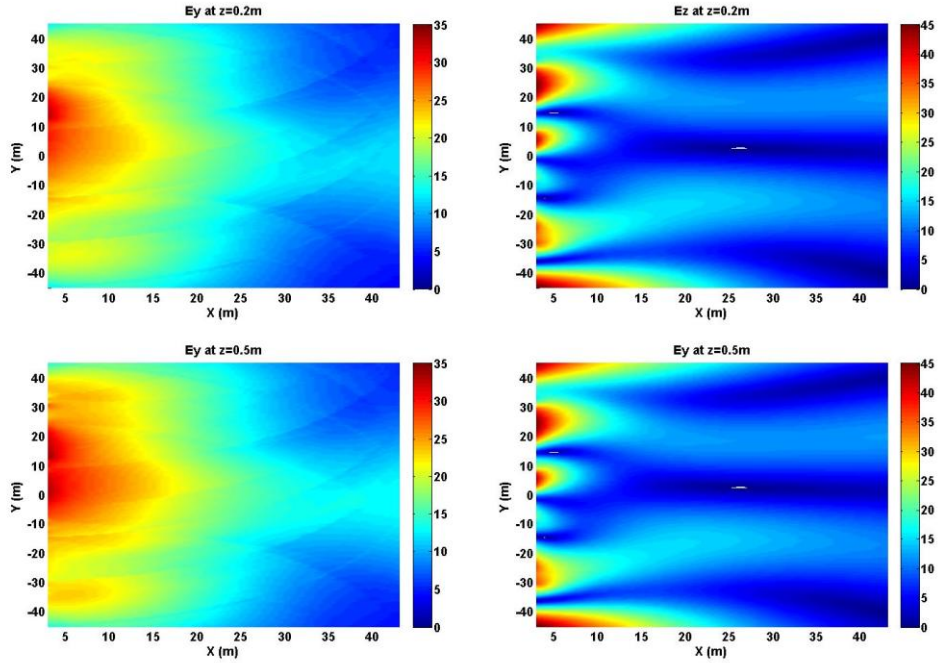

a) Height 0.2m and 0.5m above the ground

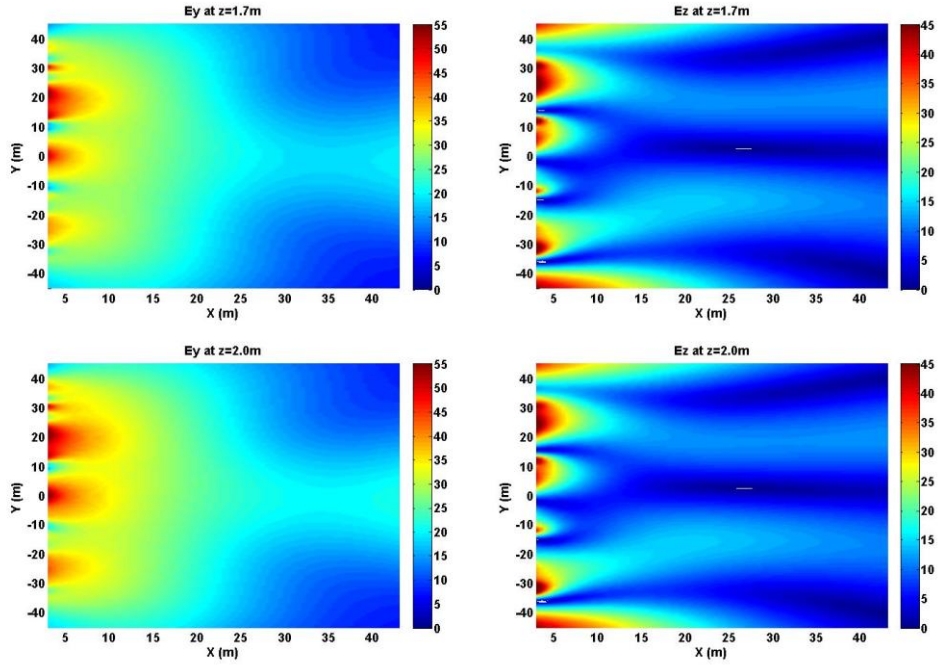

b) Height 1.7m and 2.0m above the ground

Fig 4.29 Full model with 2 °ground slope 300kW power over AVG.

Ground Condition	h[+] (m)	E-field [++] **PEC**[*]	E-field **AVG**[**]	ΔE dB (AVG/PEC))
Ey	0.2	5.6 V/m (3,0)	27.3 V/m (3,0)	**+6.9dB**
	0.5	13.9 V/m (3,0)	31.4 V/m (3,45)	**+3.5 dB**
	1.7	46.3 V/m (43,45)	53.9 V/m (3,0)	**+0.6dB**
	2.0	54.0 V/m (43,45)	58.5 V/m (3,45)	**+0.3dB**
Ez	0.2	59.7 V/m (3,45)	46.3 V/m (3,0)	**-1dB**
	0.5	59.7 V/m (3,45)	46.0 V/m (3,30.5)	**-1dB**
	1.7	59.6 V/m (43,0.5)	45.9 V/m (3,0)	**-1.1 dB**
	2.0	59.6 V/m (43,0.5)	45.7 V/m (3,30.5)	**-1dB**

Table 4.4 Peak E-field values of 300kW full scale Skelton C model on flat ground when ground conditions are PEC and AVG E-field strength value changes in PEC vs AVG ground conditions in **dB (Bold)**

* PEC: perfect electrical conduction ground
**AVG: average ground ($\varepsilon_r = 13$ and $\sigma = 0.005$ S/m)
[+]h: Height above ground (m)
[++]Location of peak shown in breaks (x,y)m

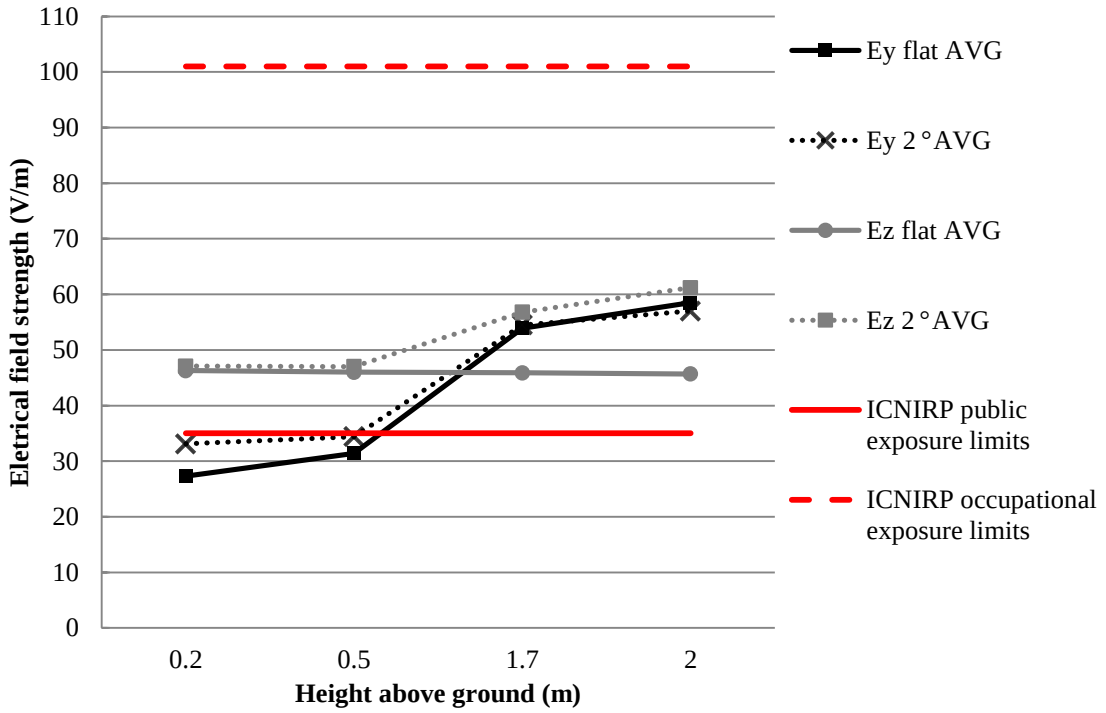

Fig 4.20 Peak Ey and Ez of full scale model above AVG at 0 °& 2 °ground slopes.

Comparing the near fields in front of the array shown in Fig 4.27 (PEC ground condition) and 4.28 (AVG ground condition), the ground reflection has a significant impact on Ey at the ankle and knee height level above the ground. The Ey strength level 5-10 m in front of array region has a 7.5dB increase when the ground conditions change from PEC to AVG. Ez was less effected having been reduced by approximately 3dB. However, this was cancelled out by an increased Ey. Comparing Fig 4.29, 2 ° ground slope model, and Fig 4.28, 0 ° ground slope model, over AVG condition the EMF has become asymmetric. The level of Ey and Ez was unchanged but the high level areas of both vertical and horizontal E-fields have expanded. Table 4.4 shows a summary of the comparison between the maximum vertical and horizontal E-field values calculated for a 2 °ground slope model. Results included PEC and AVG ground conditions. E-field strength values were calculated at 0.2m, 0.5m, 1.7m and 2.0m. Fig 4.30 compares the peak E-field values of flat AVG ground and 2 ° AVG ground from 0.2m to 2.0m above the ground with ICNIRP occupational and public exposure limits. The highest values are located a few metres in front of the array, although most of them are above the ICNIRP recommended occupational exposure limits. The actual highest EMF field level would be much lower. Although the broadcasting array

consists mainly of horizontally polarized antenna elements, the vertical E-field components are still strong in some areas of the near-field region.

4.6 Conclusions

This chapter has modeled and compared the significant parts of a high power HF broadcasting curtain array antenna. The model complexity, ground characteristics, local terrain topography, radiating power levels and array infrastructure were considered and their impacts on the near-field E-field distribution were addressed.

The HF transmission antennas usually consist of a large high power array of horizontal dipoles in front of a reflecting screen or curtain. In the near-field the vertical electric field component still presents a strong field value due to the reflection from the ground. Horizontal components show a significant increase with the height above the ground, whereas the vertical Ez component is less affected by height. Furthermore, it can be seen that it is necessary to include the supporting towers into near-field EMF strength calculations. However, it does not have a big impact on the near-field. The ground condition, local terrain topography and ground infrastructure have significant effects on the near-field field strength and distribution. Due to the joint effects of scatters (array infrastructure) and ground reflections, the horizontal components are also very high at human shoulder height. The simulated results show that the e-field in front of the array was complex and had a non-uniform distribution. The predominant field component varies from area to area. Therefore, the restrictive quantity would depend on the EMF where the human was standing. The results from CST microwave studio and NEC4 are compared with each other and show a good match for the curtain array models. CST microwave studio would be used to model a full scale transmitting site with a human phantom placed in front of the array.

Reference

[4.1] A. Hirata, O. Fujiwara, T. Nagaoka, and S. Watanabe, "Estimation of Whole-Body Average SAR in Human Models Due to Plane-Wave Exposure at Resonance Frequency," *IEEE Trans. Electromagn. Compat.*, vol. 52, no. 1, pp. 41–48, Feb. 2010.

[4.2] R. Harrington, *Field computation by moment methods*. 1993.

[4.3] "CST Mircrowave Studio Advance Guide." .

[4.4] "Numerical Electromagnetics Code NEC-4." University of California, Livermore, Ca 94551, Technical Information Dept., Lawrence Livermore National Laboratory.

[4.5] M. Jordan, "Analysis and measurement of the 'Hartley effect' in HF curtain arrays," in *IEE Colloquium on HF Antennas and Propagation*, 1995, vol. 1995, pp. 1–1.

[4.6] ITU-R RECOMMENDATION BS.80-3, "Transmitting antennas in HF broadcasting," no. 1, 2002.

[4.7] ASCE Publications, "Design of Guyed Electrical Transmission Structures," in *Design of guyed electrical transmission structures*, 1997, pp. 21–25.

[4.8] C. Gandy, "R & D White Paper WHP132," 2006.

[4.9] Y. Fu, R. J. Langley, J. M. Rigelsford, M. Hate, and J. McCalla, "The effects of local terrain topology and antenna infrastructure on simulated near-field characteristics for HF broadcast antennas," in *2012 6th European Conference on Antennas and Propagation (EUCAP)*, 2012, pp. 1218–1221.